C.P. No. 201
(16, 200)
A.R.C. Technical Report

C.P. No. 201
(16, 200)
A.R.C. Technical Report

MINISTRY OF SUPPLY

AERONAUTICAL RESEARCH COUNCIL

CURRENT PAPERS

Investigation of High Length/Beam Ratio Seaplane Hulls with High Beam Loadings

Hydrodynamic Stability Part I

Techniques and Presentation of Results of Model Tests

By

D. M. Ridland, G.I.Mech.E.
J. K. Friswell, B.Sc., and
A. G. Kurn, Grad.R.Ae.S.

LONDON . HER MAJESTY'S STATIONERY OFFICE

1955

FIVE SHILLINGS NET

C.P. No. 201

Report No. F/Res/232

September 1953

MARINE AIRCRAFT EXPERIMENTAL ESTABLISHMENT,

INVESTIGATION OF HIGH LENGTH/BEAM RATIO SEAPLANE HULLS WITH HIGH BEAM LOADINGS

HYDRODYNAMIC STABILITY PART I

TECHNIQUES AND PRESENTATION OF RESULTS OF MODEL TESTS

by

D. H. RIDLAND, G.I.Mech.E.
J. K. FRISWELL, B.Sc.
A. G. KURN, Grad.R.Ae.S.

S U M M A R Y

This report aims at providing a background, to be read in conjunction with the individual model test reports, to the hydrodynamic stability side of a research programme on seaplanes with high length/beam ratio hulls and high beam loadings.

Methods of testing and presenting results, which it is intended will be used throughout the programme, are described and points requiring further investigation are noted.

/LIST OF CONTENTS

LIST OF CONTENTS

LIST OF APPENDICES

LIST OF TABLES

/LIST OF FIGURES

LIST OF FIGURES

/Directional

LIST OF FIGURES
(Contd.)

1. INTRODUCTION

In March 1951 a detailed research programme[1] on hulls of high length/beam ratio was presented by Smith and Hamilton for discussion by the Aeronautical Research Council Seaplane Committee. It was recommended for action to Ministry of Supply and approved by the Principal Director of Scientific Research (Air).

This programme was based mainly on an earlier report by Smith and Allen[2] summarising the performance gains to be expected from the combined use of high length/beam ratio hulls and faired steps, and pointing out that considerable reduction of surface drag coefficient is thus possible, while giving the designer a much wider choice of load coefficient without sacrificing hydrodynamic performance or structural efficiency.

To assess these points quantitatively the detailed investigation of Reference 1 is divided into two main parts, aerodynamic and hydrodynamic, and the latter is further sub-divided into stability, resistance and impact tests. The stability tests are designed to show the effects of forebody warp, of afterbody length, angle and shape, and of step fairing on the hydrodynamic stability of high length/beam ratio hulls with high beam loadings. These tests are being made by M.A.E.E. in the R.A.E. Seaplane Towing Tank on the proposed series of dynamic models (Table I) and the object of this note, based on results from the first two models, is to describe and consider the test techniques, presentations of results and other factors common to this series. These observations will also form a background for results of individual model tests.

2. BASIC MODEL DESIGN

2.1. Aerodynamic

As only hull characteristics were under investigation, wing and tail design was arbitrary apart from producing a reasonably stable craft with lift and moments of the right order, and the aerodynamics of all models of the stability series were identical, as far as manufacture would allow, with those of the basic model. Aerodynamic data are given in Table II.

A 1/15 scale Sunderland wing with cropped tips was chosen for the mainplane because this section is known to have good characteristics model scale. To simulate slipstream effects, provision was made for the fitting of four compressed air driven turbine-propeller units. Leading edge slats were fitted outboard of the outer nacelles to increase $C_{L_{max}}$ and approximate to the higher Reynolds Number lift characteristics appertaining full scale. This model wing configuration (with slipstream) is shown in Figure 1.

For tests without slipstream, the nacelles and turbines were completely removed and full span slats were fitted (Figure 2). The tip slats of the previous configuration were insufficient by themselves to remove a kink from the lift curve[3], which was presumably due to the low Reynolds Number at which the test was made.

The tailplane was that of a 1/15 scale Sunderland apart from the elevators, the chord of which was increased to give better coverage of the attitude range and improve aerodynamic stability. This effective increase in tail area does not apparently alter the lower critical trim, i.e. the trim of a point on the lower stability limit[4]. The position of the tailplane, high on the fin (Figure 3), was chosen to avoid interference from spray at high planing attitudes.

The fin and rudder were combined in one vertical surface, but moments could be induced by the bending of a metal tab slotted into the trailing edge.

/With

With a keel attitude of zero degrees, the S.M.C. quarter chord point was 0.04 feet forward of and 0.28 feet above the C.G. (Table II). The model was thus aerodynamically stable, having a stick fixed static margin of approximately 0.15 c in the case without slipstream.

2.2. Hydrodynamic

The hydrodynamic investigations were made by making successive variations on the basic hull form while retaining the same forebody length and beam. The methods used to obtain the hull lines for each model of the series were, apart from the changes in afterbody shape, and step fairing, essentially similar; they are described in Appendix I and hull lines for the basic model (Model A) are given in Figure 4.

In order to produce clean breakaway of spray, model scale, with negligible effect on stability, chine strips were fitted to all of the model hulls. They consisted of strips of foil inserted along the chine so as to bisect the hull wall-planing bottom angle and stand proud to the order of 0.003 inches[5].

3. TEST TECHNIQUES

The tests to be carried out on each model of the series are assessments of,

(i) aerodynamic lift,

(ii) hydrodynamic longitudinal stability,

(iii) spray, and

(iv) hydrodynamic directional stability.

Within this framework, model parameters such as beam loading are varied to suit the needs of the programme.

The apparatus used in the R.A.E. Seaplane Tank, including the various rigs and the general methods of testing, is described in Reference 3. Briefly,

(i) the lift is assessed by making constant speed runs with the model in the lift rig at fixed incidences clear of the water and measuring the lift;

(ii) the hydrodynamic longitudinal stability is determined by making constant speed runs at different elevator settings over a range of speeds, with the model free in pitch and heave;

(iii) the spray is observed and photographed, mainly over the displacement range of speeds during the longitudinal stability tests, and

(iv) the hydrodynamic directional stability characteristics are observed with the model free in pitch, heave and yaw, by yawing the model to starboard through about 20 degrees at constant speeds.

Ideally these tests would be carried out completely on an actual aircraft of about 10,000 lb. weight when the complications of scale effect would be greatly reduced, but for reasons of expense and time this cannot be done.

/A

A proposal has been made, however, for a research aircraft of this size[6], on which a selection of the tank tests can be repeated, thus making an evaluation of the worst scale effects possible. Meanwhile, the model test techniques are designed to simulate as near as possible full scale conditions. The lift assessment is subsidiary in that it is made mainly to ensure the correct load on water during the stability tests. The longitudinal stability test runs are made (a) without and (b) with disturbance. The former is intended to simulate full scale conditions of calm sea and no wind, while the latter is to represent the rough sea or wave case. Model spray is complex from the scale effect point of view, but direct scaling up has been found to give a good idea of what might be expected full scale[7] for the calm water case; to simulate spray in waves would be too expensive and time taking for the information obtained. The directional stability tests are known to give answers which are liable to a large scale effect but, owing to lack of full scale data, this has never been determined quantitatively. The tests, however, do show which hull form is better from the directional standpoint. These points are amplified below and particular attention is paid to any modifications or additions to the methods of Reference 3.

3.1. Aerodynamic lift

Runs were made at constant speeds with the model at fixed incidences and the lift measured.

In the slipstream case, turbine speed was set to give a reasonable take-off propeller thrust, and was held constant over the take-off speed range. The curve of model thrust against velocity coefficient is given in Figure 11. Lift runs were made with a range of incidences at each of several speeds, with elevators central. Without slipstream, i.e. with a clean wing and full span leading edge slats, a range of incidences was covered at two speeds, to check Reynolds Number effects. This was repeated with the slipstream configuration, propellers windmilling, to represent the landing case.

The effect of elevator angle on the lift was then checked by repeating the foregoing at different elevator settings. This was justified by the large elevators and the comparatively large changes in lift that were found.

To complete the lift data, a tailplane lift curve was obtained by repeating the case without slipstream, but with the model tail unit removed.

Throughout the lift runs the model was suspended so as to keep the mainplane at a constant height, about 1.5 c above the water surface. No allowance was made for ground effect, but earlier work on this subject by Clark and Tyc[8], using a model with an unslatted wing, shows an error in C_L value at 10 degrees wing incidence (wing chord to horizontal) of about 4% (using values of height above water corresponding to the present case). The error is zero at 4 degrees incidence, and approximately linear up to $C_{L_{max}}$ which is unchanged by ground effect. In the present hydrodynamic stability tests, therefore, at 16 degrees incidence, corresponding generally to upper limit attitudes, one can expect to have actual lift values of the order of 8% greater than those at similar attitudes obtained by measurement in the lift rig.

The lift curves are used primarily for estimation of load on water, so the maximum error will be found at take-off speeds with high attitudes. At increasing distances from this region of the stability diagram it will be progressively less. If the curves are used for any theoretical treatment a correction for ground effect can be made to the slope.

/The

The ground effect problem in the Seaplane Tank needs re-checking at the higher C_L's currently obtained by using full span leading edge slats and, as the increase in slope of the lift curve on approaching the ground may be expressed as roughly equivalent to an increase in aspect ratio, it may be possible to devise a set of generalised correction curves having only negligible error.

3.2. Hydrodynamic longitudinal stability

For the longitudinal stability determination constant speed runs were made with different elevator settings, over a range of speeds from 4 to 40 feet per second. The model was towed from the wing tips on the lateral axis through the C.G., being free in pitch and heave only. The speed, elevator angle, trim, spray and stability characteristics were noted. On all runs where possible a 5 degree nose down disturbance was applied and the stability characteristics were again noted, but this was sometimes prevented by the violence of the instability occurring on the undisturbed run, and by the model becoming airborne when disturbed. Only take-offs were simulated, and each run was made with a smooth undisturbed water surface, using zero flap and one C.G. position. In each case the motion was defined as unstable when the resulting oscillation (if any) was apparently divergent or had a constant amplitude of 2 degrees or more. This 2 degree limit has been chosen arbitrarily as the maximum permissible for safety under operational conditions[9]. It was found that in the majority of cases of instability, the oscillation maintained a constant amplitude and this could be read to within 5%. On plotting these observations the unstable part of the diagram could be divided into natural regions of equal steady oscillations as in Figure 5. Similar diagrams for each model should help in understanding and correlating the stability of this series, but in general individual test points with amplitudes will be given and no zones will be drawn.

3.2.1. Undisturbed case

The model longitudinal stability case with no disturbance (it could be called the ideal case, inasmuch as the greatest possible number of unknowns is eliminated) has been given a fundamental theoretical treatment by Perring and Glauert[10] and is in consequence fairly well understood. Several simplifying assumptions were made, one of which was that in the case of lower limit (forebody) instability, the seaplane could be represented hydrodynamically by a single flat planing surface of finite width. Under these conditions the theory has been found to give good quantitative agreement with experiment when correct values of the stability derivatives are used[9,11]. In the case of upper limit instability (two step porpoising), the seaplane is considered equivalent to two flat planing surfaces in tandem, but the effects of the forebody wake on the afterbody are neglected. The theory thus becomes more qualitative than quantitative in this case.

In the present tests, on models with high beam loadings and a correspondingly increased tendency towards chine immersion*, the application of Glauert's theory may be queried. The main point about chine immersion is that, at fixed incidence, when it occurs the aspect ratio of the planing surface starts changing, giving a discontinuity in the slope of the lift curve for that incidence, at the point of chine immersion[12]. From general considerations, it would appear that the theory is just as valid in this

/case

---

* Chine immersion - In this report it has been assumed that chine immersion occurs when the point at which the forebody chine and transverse (or equivalent transverse) step intersect, lies below the undisturbed water surface plane. This is not strictly true, but it provides a convenient basis on which to work (see Reference 22).

case as it is in that of flying boats with beam loading coefficients of the order of 1.00. The theory is based on flat plates, which have maximum chine immersion, and has been applied in cases where there is little or no immersion, giving good results. It is felt that stability calculations in the vicinity of the lift slope discontinuity could be avoided and good limits could still be obtained.

The full scale longitudinal stability limits to which undisturbed model limits correspond, are those obtained in conditions of no wind and dead calm sea. Unfortunately, a dead calm sea is of such infrequent occurence that it cannot economically be waited for. Normal full scale stability limits are therefore determined in a sea having waves less than about 9 inches high and either negligible or no swell, with wind speeds of less than 5 knots for research investigations, or 10 knots for routine tests.

3.2.2. Disturbed case

In the case of stability with disturbance, no theory, or modification of the above theory, has yet been advanced and the phenomenon is not so well understood.

Disturbance techniques for stability testing have been used in the R.A.E. Seaplane Tank for some time. In 1936[13] it was the practice to do test runs while the water surface was still disturbed from the previous run. If instability did not develop the model was "disturbed fairly violently" and the subsequent motion was observed. A more detailed technique was necessitated by the fact that two seaplanes, the Lerwick and the Saunders-Roe R4/33, stable model scale, became unstable full scale, the latter crashing as a result of this instability. This revision of technique is reported by Gott[14] who states that "a serious difficulty appears when it is necessary to decide what is a suitable disturbance to give the model" and that "it has always been generally agreed that the model disturbance should be correctly scaled down from the maximum disturbance the full scale flying boat can receive in service". It was found that a nose down disturbance was more effective in producing instability than a tail down disturbance of equal magnitude and that a train of about six waves could cause the onset of instability, even though they were waves of small height, as long as the wave length was of the right order to produce a resonance effect. It is concluded (in Reference 14) that the wave technique is too time consuming and that a suitable manual disturbance must be given to the model. This disturbance must not be too small in case an unstable region is missed, and it must not be too large, so that the aircraft under consideration is not unduly penalised, i.e. so that the stability of the aircraft is not made to appear worse than it is under normal operating conditions. Some time later, in 1944[9], Smith describes the disturbance given as a severe nose down angular displacement of the order of 10° amplitude and, in the more recent tests on the Saunders-Roe E6/44[15], the applied disturbances were of the general order of 6° - 8° nose down, except at fine angles of trim when the keel attitude was lowered to 0°, i.e. the disturbance was less than 6°. It is clear from the foregoing that the degree of disturbance given is a compromise and that the significance of applying a given degree of disturbance needs further investigation. This has been done, in a limited manner, and is considered in the next two paragraphs.

3.2.3. Stability limits with disturbance

The effect of disturbance in the initially unstable region is to produce a sudden increase in the amplitude of steady porpoising. It follows that there must be a critical disturbance in this region, such that, if it is exceeded, the model will oscillate at the higher amplitude. Further, as

/the

the degree of disturbance is increased, so is the unstable region until a limit is reached when no further instability can be induced regardless of the disturbance. Partial limits for 0, 3, 4, 5, 6 and greater degrees of disturbance for Model A are shown in Figure 6. A complete set of graded stability limits could have been obtained, but this was considered unnecessary.

An investigation by Locke and Hugli[16] into disturbance effects, restricted to a particular part of the stability diagram, substantiates the existence of different limits for different degrees of disturbance and that there is a final limit which further increases in magnitude of disturbance do not alter.

3.2.4. Wave - disturbance correlation

The disturbance technique was evolved mainly to simulate full scale conditions in waves without the expense of time or labour incurred by producing waves in the tank. It is suggested that the impact of a hull on a wave front, or a series of wave fronts assuming a cumulative effect, could be considered as tantamount to a given degree of disturbance and conversely a given disturbance could be matched by one or more wave systems. By taking (model scale) several points within the 5 degree unstable region but outside the undisturbed unstable region, it was possible to determine for each point the critical nose down impulsive disturbance, i.e. the smallest disturbance which would induce instability, and relate it to a number of wave trains which would similarly just induce instability. This was done by making steady speed runs through waves of selected length/height ratios and, in each case, effectively increasing the wave height while keeping the ratio constant until instability set in. The number of such wave systems so related to one disturbance at a given point in the stability diagram is infinite, lying along a well defined narrow band which could, for practical purposes, be taken as a curve. The points chosen for investigation, with the corresponding curves, are shown in Figures 7a and 7b respectively. (Normal stability diagram notation is used for points in Figure 7b).

From this limited investigation several tendencies are apparent. It seems that for a given wave length/height ratio, as attitude is decreased so the wave height necessary to induce instability increases and, as speed is increased, the wave height necessary for instability increases, the effect of wave height being less marked as the wave length/height ratio is increased. Perhaps the most important point is that a stability limit obtained by applying a given degree of disturbance does not necessarily represent any particular full scale limit obtained in a given wave system. For instance, suppose it were desired to assess the stability of a full scale version of the model (weight 150,000 lb. and beam 9.5 feet) in waves of length/height ratio 50:1 and height 2 feet = 0.21 b. Then, ignoring scale effect, from Figure 7b cases 1, 2 and 3 would be unstable while cases 4 and 5 would be stable. The 5 degree limit (Figure 7a) is obviously incorrect as it embraces all the points; similarly with a $4\frac{1}{2}$ degree limit (from the critical disturbances of Figure 7a). A 4 degree limit would render point 2 stable, and a $3\frac{1}{4}$ degree limit would do likewise for points 1 and 2. while a 3 degree limit, or lower, would make the points all stable. Limits have been considered over a range from complete instability to complete stability for the five points and no satisfactory correlation has been obtained over the whole speed range with the wave effects. From the shape of the curves in Figure 7b, it can be seen that this argument can be applied to any of the wave systems considered other than those rendering the five points all unstable or stable, although the divergence in stability lessens with increasing wave length/height ratios. The critical disturbances were assessed to within $\frac{1}{2}$ degree and the wave systems were accurately checked.

/That

That points 4 and 5, with critical disturbances of 3.0 and 3.5 respectively, lie close to the 5 degree limit, as possibly due to an inaccuracy in the limit in that region. The difficulty lies in giving an impulsive disturbance of exactly 5 degrees to the model without duplicating runs and in that region the stability of Model B was very sensitive to the magnitude of the disturbance, porpoising amplitudes increasing rapidly as the limit was exceeded. It may be that the disturbances were slightly less than 5 degrees in amplitude, as great care is needed in this high speed lower limit region to avoid submerging the nose of the model, but this in no way detracts from the foregoing argument.

Any technique evolved to exactly simulate, by means of disturbance, full scale stability in a given wave train will be laborious and the time taken will be prohibitive. Future tests with disturbance will be made with an amplitude of disturbance greater than critical (about 7 degrees generally), when the worst stability diagram will be obtained. After making any necessary allowance for scale effect, this limit will represent the worst stability case in any wave system. As the wave height or length/height ratio decreases, so will these limits tend to the calm water or undisturbed limits.

An alternative method would be to produce in the tank the scaled down waves in which the boat will have to operate and then obtain a stability diagram without disturbance. This method would again be time taking, but if the full scale technique of accelerated runs with fixed elevator is feasible in the tank, the tank time will be considerably reduced, although analyses of necessary recordings will slow things down. When dealing with waves in the tank, Reference 17 should be consulted on wave stability and wave maker limitations.

A wave check, similar to the foregoing, carried out at one point for Model A (which differs geometrically from Model B only in respect of forebody warp) showed no difference from the corresponding results of Model B. It seems reasonable to assume therefore that, for models of this series at the same weight, if any major change in wave effects is brought about it will be mainly due to afterbody alterations. Occasional wave checks, during the programme, coupled with the two limiting stability diagrams, should give the optimum amount of information for the time spent.

3.2.5. Recording systems

As a further aid in stability testing two desynn systems were attached to the model rig, one for height using a flap type transmitter, and the other for attitude using a miniature transmitter. Rapid response indicators were used and these were fitted in an automatic observer which, by means of a Bell and Howell A.4 cine camera, also recorded time and speed. The systems have the normal desynn limitations[18] but the required working frequencies, 3 or 4 per second, are low and, as the indicators are damped, the trends of height or attitude changes are fairly well shown. Two examples are given in Figure 8 (a) and (b). In (a) a disturbance at 28 feet per second, C_V = 7.16, elevator -8 degrees is shown. The observed amplitude of porpoising was 8 degrees and this agrees well with the recorded amplitude. In (b) the model is running at a steady speed of 26 feet per second, η = -8 degrees, through a wave train of length/height ratio 110:1 and wave height 0.25 beam. Calibration of the attitude system is rather tedious but this could easily be overcome, if necessary, by a modification which would slightly increase model inertia.

/It

It is interesting to note, in view of paragraph 3.2.4., that, in the two examples given in Figure 8, although the test conditions were the same in each case, the recording with disturbance shows no similarity to the recording with waves. The frequencies and amplitudes of oscillation, as well as the changes in C.G. height show marked differences. A detailed investigation along these lines over a range of wave length/height ratios with wave heights sufficient to produce instability, would be time taking, but it should be done if possible.

3.3. Spray

In an attempt to get spray photographs of reasonable comparative value F.24 cameras were positioned off the starboard bow, the starboard beam forward of the wing and the starboard beam aft of the wing. A chequered pattern, consisting of alternate black and white squares of 1/4 beam side, with the step point as origin, was painted on the starboard side of the model to aid in subsequent analysis. An exposure time of $\frac{1}{50}$ of a second was used in order to get photographs of apparently continuous spray envelopes instead of the discrete drops without sense of direction, which result from using say an electronic flash with an open camera shutter. As the cameras are close to the model, the depth of focus is small and roughly only one plane, chosen as that containing the grid on the hull side, could be in focus. The photographs therefore will show parts of the spray and model wing as being considerably out of focus, but against the chequered background the spray profile is sufficiently well defined for a reasonable comparison to be made.

The photographs were taken simultaneously during the undisturbed longitudinal stability assessments, with η = -8 degrees, mainly over the displacement range of speeds. An example is given in Figure 9.

3.4. Hydrodynamic directional stability

For the directional stability assessment the model was towed and pivoted at the C.G. so that it was free in pitch, yaw and heave. A constraint was applied in roll so that subsequent analysis and comparison would not be unduly complicated. Further, as full scale take-offs are made as near into wind as possible, ailerons are effective at low speeds and the wings are normally held level by the pilot. The roll constraint thus gives a good first order simulation. The effect of roll constraint on directional stability was checked and found to be negligible. It was felt that the effect of change in weight would be of similarly small order. This has since been checked at one other weight on Model C and the resulting slight change in directional stability can, for practical purposes, be ignored. Both of these effects will be discussed in the relevant model reports.

Steady speed runs were made over a range of speeds from 4 to 40 feet per second. At each speed the model was yawed in steps up to not more than 18 degrees, moments being applied through strings attached to the wing-tips level with the C.G. The direction and order of magnitude of the resulting hydrodynamic moment was judged by the operator through the pull in the strings, and the angle of yaw was read off a scale on the tailplane with an accuracy of about $\pm \frac{1}{2}$ degree. This type of test was carried out on a dynamic model of the Princess[19] but owing to the large undetermined scale effect it was stated to be somewhat inconclusive.

When the model is yawed the water flows over the hull side presented to the direction of motion (the port side in the present case) and, at the larger angles of yaw and higher speeds, it sticks and covers the whole of the side for the length of the afterbody sometimes running up

/the

the vertical tail surface. It was felt that this effect would not be so severe full scale, so about six forward sloping strips of thin triangular section were stuck along the affected part of the afterbody wall to deflect the water[3, 19], and the tests were repeated with this model configuration. The effect of attitude was checked by doing the foregoing at two elevator settings, +2 and -10 degrees.

All of the aforementioned tests have not been done on each model; in particular, recordings have been restricted to isolated cases. Those tests done on any model will be indicated in the relevant model report.

4. PRESENTATIONS

The majority of the test results for this series of models are presented in non-dimensional form. If, however, a flying boat of 150,000 lb. and 9.5 feet beam be envisaged (as per Reference 1) the models are then 1/20th scale and a quick idea of full scale values may be obtained by multiplying velocity coefficient C_V by 10.35 giving knots and load coefficient C by 54,600 giving pounds.

4.1. Aerodynamic lift

The lift curves without slipstream have been plotted in the normal manner. An example showing the effect of elevator is given in Figure 10. The points plotted are check points in respect of which the curves have been modified from those of the first wing tested. The tailplane lift curve is shown in Figure 12 and lift curves with slipstream have been plotted at different thrust coefficients, T_C, Figure 13.

None of the curves have been corrected for ground effect, this being considered unnecessary from a comparative hydrodynamic point of view.

4.2. Hydrodynamic longitudinal stability

The longitudinal stability diagrams with and without disturbance are presented as in Figures 14 and 15 respectively. No flying region is indicated because, except at the lower weights and with slipstream, the models did not fly, but a good idea of flying speeds for each elevator setting can be obtained from the corresponding load coefficient diagrams when $C_{z_1} = 0$, e.g. Figure 22.

The limits only (and not the complete diagrams) are presented non-dimensionally on a speed base, and on a draught base (Figure 16). Curves of load coefficient, C_Δ, against velocity coefficient, C_V, necessary for the second type of stability picture, are included.

The limits on a velocity coefficient base are straightforward and require little comment (Figure 16a), but a short explanation on the derivation of the draught base should be useful and is given below.

The idea of plotting stability limits on another base was originally considered from the point of view of obtaining a collapse, thereby saving time, and the base used was C_{z_1}/C_V. This was used by Locke in his method for the interpolation of stability limits[20], where it is suggested that by suitable modification of the scales one generalised set of limits, on a C_{z_1}/C_V base, will serve for different weight and wing conditions on the same hull. Conversely, then, one might expect a complete collapse of limits for several weights on the same hull when plotted on a C_{z_1}/C_V base. This is stated to be the case by Whittley and Crewe[21] but

/that

that it is only partially so can be seen from Figure 16b. The failure to collapse may be accounted for by the fact that Locke's analysis is based on hulls with beam loadings of the order of 1.00, when Froude number effects can be neglected at higher speeds, and the present series of hulls, with beam loadings of the order of 2.75 and consequent higher draughts, give rise to Froude number effects which cannot be ignored. This, however, is only a suggestion and has not been proved.

When attitude is fixed, $\sqrt{C_\Delta}/C_V$ is proportional to draught, but in the stability case, with varying attitude and consequently varying aspect ratio, $\sqrt{C_\Delta}/C_V$ does not represent draught. To find a draught base which is suitable for stability plotting, use was made of data from a report by Perring and Johnston[22]. The two planing cases, without and with chine immersion, are considered.

Case I - without chine immersion

In this case the forebody of the model is considered as an ideal planing wedge (Figure 17) of infinite beam in so far as the maximum beam is never wetted.

Assume a hydrodynamic lift coefficient, k_L, defined by

$$\Delta = \rho_w V^2 S_1 k_L$$

$$= \rho_w V^2 S_1 a_1 \alpha_K$$

where S_1 is the projected still water planing area on a plane containing the tangent to the forebody keel at the main step (Figure 18) and the relevant aspect ratio A_1 is defined as $A_1 = \frac{b_w^2}{S_1}$ where b_w is the wetted beam. Expressing S_1 and A_1 in terms of draught, d, and attitude, α_K, we get

$$S_1 = \frac{d^2}{\sin \alpha_K \cos \alpha_K \tan \beta}$$

$$\text{and } A_1 = \frac{4 \tan \alpha_K}{\tan \beta} .$$

Over the attitude range considered, α_K is small, so it can be assumed that $\sin \alpha_K = \alpha_K$ and $\cos \alpha_K = 1$. The projected area and aspect ratio expressions then become

$$S_1 = \frac{d^2}{\alpha_K \tan \beta} \quad \text{and } A_1 = \frac{4 \alpha_K}{\tan \beta} .$$

From reference 21, a_1, the slope of the lift curve, is a function of the aspect ratio and can be expressed as

$$a_1 = C_\beta \cdot A_1^{0.53} = C_\beta \left| \frac{4 \alpha_K}{\tan \beta} \right|^{0.53}$$

where C_β is a coefficient, depending on the deadrise angle β, (see Figure 19, reproduced from Reference 21).

/Returning

Returning to our original base and substituting we have

$$\sqrt{\frac{C_\Delta}{C_V}} = \sqrt{\frac{\Delta}{\rho b^3}} \cdot \sqrt{\frac{gb}{V^2}}$$

$$= \sqrt{\frac{\rho_W V^2 S_1 a_1 \alpha_K}{\rho b^3} \cdot \frac{gb}{V^2}}$$

$$= \sqrt{\frac{d^2 \alpha_K}{\alpha_K \cdot \tan\beta \cdot b^2} \cdot C_\beta \cdot \left[\frac{4 \alpha_K}{\tan\beta}\right]^{0.53}}$$

$$= \frac{d}{b} \sqrt{\frac{C_\beta}{(\tan\beta)^{1.53}} \cdot (4\alpha_K)^{0.53}},$$

$$\text{therefore } d = b \sqrt{\frac{(\tan\beta)^{1.53}}{C_\beta}} \cdot \sqrt{\frac{C_\Delta}{C_V}} \cdot \frac{1}{(4\alpha_K)^{0.265}}.$$

The mean deadrise angle for the wetted part of the forebody of the model now under consideration can be taken as 28°, in which case $C_\beta = 0.36$ and $\tan\beta = 0.5317$. With beam, $b = 0.475$ feet, the draught expression simplifies to

$$d = \sqrt{\frac{C_\Delta}{C_V}} \cdot \frac{0.338}{\alpha_K^{0.265}} \text{ feet} \quad \ldots \quad \text{with } \alpha_K \text{ in radians.}$$

It differs from the original base in that an attitude function has been brought in. This function, $\alpha_K^{0.265}$, is plotted in Figure 20 to simplify the transformation of the stability limits from a velocity coefficient to a draught base.

Case II - with chine immersion

This differs from Case I in that the maximum beam, b, of the representative wedge is always wetted. The lift equation is unaltered in form,

$$\Delta = \rho_W V^2 S_2 a_2 \alpha_K$$

but S_2, again the projected still water planing area on a plane containing the tangent to the forebody keel at the main step, becomes now, instead of a simple triangle, a triangle plus a rectangle, the size of the latter depending on the extent to which the chines are immersed (Figure 18). The corresponding aspect ratio A_2 is defined as $A_2 = \frac{b^2}{S_2}$.

If $(1-\gamma)s$ is the length of chine submerged and s is the wetted length of the keel, then, assuming as before that $\sin\alpha_K = \alpha_K$ and $\cos\alpha_K = 1$,

$$\gamma s \alpha_K = \frac{b}{2} \tan\beta \text{ and } s = \frac{d}{\alpha_K},$$

/whence

whence $\gamma = \frac{b}{2} \cdot \frac{\tan \beta}{d}$,

$$S_2 = \frac{bs}{2}(2-\gamma)$$

$$= \frac{b}{4\ \alpha_K}(4d - b \tan \beta),$$

$$A_2 = \frac{4\ b\ \alpha_K}{4d - b \tan \beta}$$

and $a_2 = C_\beta\ A_2^{\ 0.53}$.

Reducing as in Case I we have

$$\frac{\sqrt{C_\Delta}}{C_V} = \sqrt{\frac{\rho_w V^2\ S_2\ a_2\ \alpha_K}{wb^3} \cdot \frac{gb}{V^2}}$$

$$= \sqrt{C_\beta\ \alpha_K \left[\frac{4d - b \tan \beta}{4\ b\ \alpha_K}\right]^{0.47}}$$

$$= \sqrt{C_\beta\ \alpha_K \left[\frac{4d - b \tan \beta}{4\ b\ \alpha_K}\right]^{1/4}} \quad \text{approximately,}$$

therefore $\left[\frac{\sqrt{C_\Delta}}{C_V}\right]^4 \frac{4\ b\ \alpha_K}{C_\beta^{\ 2}\ \alpha_K^{\ 2}} + b \tan \beta = 4\ d.$

Substituting for C_β and $\tan \beta$, and simplifying gives

$$d = \left[\frac{\sqrt{C_\Delta}}{C_V}\right]^4 \frac{3.65}{\alpha_K} + 0.0635 \text{ feet} \quad \ldots \text{ with } \alpha_K \text{ in radians,}$$

$$= \left[\frac{\sqrt{C_\Delta}}{C_V}\right]^4 \frac{209.2}{\alpha_K} + 0.0635 \text{ feet} \quad \ldots \text{ with } \alpha_K \text{ in degrees.}$$

The above analyses are based on the assumption that a flying boat can be represented by a planing wedge. The draught bases derived are therefore only valid when planing conditions have been established, when there is no interference from the afterbody and when the wetted part of the keel is straight, i.e. at lower limit attitudes generally. Draught is not normally measured during stability tests and the only check which could be obtained was by measuring the draught from spray photographs.

Comparison of measured and calculated draughts

α_K	C_V	C_Δ	$\sqrt{C_\Delta}/C_V$	draught d ins.		error ins.
				measured	calculated	
8.7	9.0	1.13	0.118	0.65	0.79	0.15
9.0	7.03	1.82	0.192	1.00	1.27	0.25
8.9	7.21	1.02	0.140	0.75	0.91	0.15
8.2	9.21	0.315	0.061	0.25	0.41	0.15
8.6	8.18	1.2	0.134	0.80	0.90	0.10
8.2	10.0	0.72	0.085	0.45	0.59	0.15
8.5	7.98	1.50	0.154	0.75	1.02	0.25
8.8	8.24	0.65	0.098	0.40	0.65	0.25
				Mean error		0.18

/These

These photographs were taken with the model at high attitudes when there was almost certainly some form of afterbody interference, i.e. the afterbody may have been planing or it may have been struck by spray from the main step. Either of these effects would reduce the forebody load on water and make the calculated load coefficient too high, which in turn, would give high values of draught.

It can be seen from the table that the calculated draughts are high.

There is a mean positive error of 0.18 inches and around this there is a maximum scatter of 0.08 inches. The mean error could be due, in addition to incorrect values of load coefficient because of afterbody interference, to the use of an incorrect value of deadrise coefficient, C_β, as the model used had a forebody warp of 4 degrees per beam, or to the ignoring of splash up in the definition of wetted area. The scatter can easily be accounted for by the method used to obtain draughts from the spray photographs. It is felt that with a more detailed investigation the major error could be eliminated, when the formulae will give draughts as accurately as they can now be obtained by direct measurement on the stability rig. The draught formulae will, of course, be just as applicable full scale as they are model scale, providing that the correct values of $\sqrt{C_\Delta}/C_V$ can be obtained.

The lower stability limits for Model B are plotted on a draught base in Figure 21. As, according to our earlier definition, chine immersion will occur at draughts above $d = 0.5\ b \tan\beta = 1.52$ inches, the formula used was that without chine immersion. The stability limits are transformed into a family of straight lines, which converge regularly as draught decreases. (The lower draughts are at the right hand side in conformity with the previous limit plots). The lower weight limit, $C_{\Delta_0} = 2.00$, does not appear to belong to the family, but as it lies mainly outside the limits of application of the formula, in that the curved part of the forebody keel is wetted and the forebody can no longer be represented by a simple wedge, it can be neglected when considering the method of plotting. It can be noted, however, that if all the curves were extended to $a_K = 0$, the maximum draught error would be 0.05 inches, and the overall change in draught along the lower limits is only about 0.3 inches.

The aim here has been to establish the method and its validity. The implications of this type of plot and its possible modification, in the light of more recent American wedge data, will form the subject of a later note, when more of the present series of model stability tests have been completed. In all the individual model reports longitudinal stability limits will be presented both on a C_V base and on a draught base.

In obtaining the previously considered lower limits, increases in model weight were effected by adding weights to the C.G. bar, i.e. by keeping the moment of inertia relatively constant and decreasing the radius of gyration. This approximates to the full scale case and changes in moment of inertia have little effect on stability limits over a wide range when the limits are found by means of constant speed runs[23]. It is felt however, that the variation of critical trim with mass, moment of inertia and radius of gyration requires further investigation on these high C_Δ models.

The foregoing examples have been based on longitudinal stability limits without disturbance, but limits with disturbance are presented in the same manner.

A typical load coefficient diagram is shown in Figure 22. The curves, which correspond to trim curves on the stability diagram at the same C_{Δ_0} are corrected for elevator effect.

/4.3. Spray

4.3. Spray

The spray characteristics of any of the models at a given speed can best be assessed by inspection of the spray photographs for that speed. By suitable analysis the co-ordinates, x, y, z, of a peak on the spray blister have been obtained for each of the speeds 4, 8, 12 and 16 feet per second. At higher speeds the spray peak is blanketed by the wing. The locus of these points has been plotted in Figure 23 for Model B at $C_{\Delta_0} = 2.50$ using the non-dimensional co-ordinates C_X, C_Y and C_Z with the step point as origin. This line gives a good overall idea of the model spray characteristics at a given weight and will form a convenient basis for comparison. If it is desired to use any of the more involved N.A.C.A. spray co-ordinates such as $C_X/C_\Delta{}^{1/3}$, (Reference 24) sufficient information will be found in each model report.

4.4. Directional stability

Unlike the longitudinal stability diagram which is divided into definite stable and unstable zones, the directional stability diagram, with degrees of yaw as ordinates and velocity coefficients as abscissae, represents a plane of instability which is crossed by lines of both stable and unstable equilibrium. If the model is positioned (in effect) at any point in this plane and then given complete freedom at constant speed, it will swing round to the nearest line of stable equilibrium that it can reach without crossing an unstable line. In other words, it will swing towards a line of stable equilibrium and away from a line of unstable equilibrium. The present tests have been made with no rudder tab, i.e. with zero aerodynamic yawing moment, and the directional stability diagrams are for this case only. Similar diagrams could have been obtained for different rudder settings, but they are not necessary to the present investigation and it is considered that they would differ by very little from the zero yawing moment case.

The first directional stability diagram (Figure 24) has been obtained for Model A with an elevator setting which gives a stable low take-off trim, and explanatory notes, based on observation, have been added. The second diagram (Figure 25a) corresponds to stable high take-off trims. It can be seen that pitch changes have little effect on the directional stability except at high speeds, and even there the effect is insufficient to warrant separate investigations. The remaining models have thus been tested at one elevator setting only.

It has been suggested that, although the aforementioned diagrams are useful for a model to model comparison, because of the large scale effect (completely undetermined through lack of full scale data), model directional stability tests should be repeated with side breaker strips[3] in position and the two sets of diagrams so obtained represent limiting conditions between which the full scale cases lie. This has been done in the high attitude case and the results are given in Figure 25. This shows that the stable equilibrium line is substantially unaltered up to $C_Y = 3$ and it is then coincident with the speed axis. The breaker strips intended to prevent the flow from sticking to the after hull side functioned well in this respect, but in view of the fact that only an exact reproduction of part of the normal stability diagram is obtained by this type of test, i.e. the curve below $C_Y = 3$, it has been discontinued.

A much better idea of the nature of directional stability diagrams could be obtained by yawing a small model through 360 degrees. This is not completely devoid of practical significance, particularly at lower speeds. A pilot using reversible pitch propellers could easily overcorrect and in the limit a flying boat might well be driven backwards when manoeuvring.

Most of the models in this programme will thus be tested directionally at one weight, one C.G. position, one elevator setting and one rudder setting, without breaker strips. Results will be presented in the form of Figure 25a.

/4.5. Elevator

4.5. Elevator effectiveness

As the aerodynamic characteristics of each model are the same, the effect of changes of hull parameters, such as forebody warp, on elevator effectiveness can easily be ascertained. Corresponding to each model weight therefore a plot of elevator effectiveness in take-off will be given. The analysis has been done in some detail because the curves of attitude against elevator angle obtained were of definite form and had little scatter. The method used is illustrated in Figure 26 (a), (b) and (c). Figure 26(a) is a plot of attitude against elevator angle for a given speed, (b) is the slope of this curve together with the mean ordinate and (c) is the final graph showing the variation of elevator effectiveness with velocity coefficient.

5. CONCLUDING REMARKS

The test techniques employed throughout the hydrodynamic stability part of the advanced hull design investigation will be as laid down in this report. In the case of the disturbance technique however, it is often impossible to give large disturbances at the high speed end of the lower limit region and we are still left with the operator's opinion of what is a reasonable disturbance under the circumstances. The technique is essentially an estimation of the ability of the flying boat to operate in waves. If with disturbance, a good set of undisturbed stability limits closes up and the stable region completely disappears, then the boat is useless in rough water; on the other hand, if the disturbed limits differ only slightly from good undisturbed limits, the boat will handle well in rough water. In the present tests it is proposed to give sufficient disturbance to the model to obtain the worst possible limits, subject to safety considerations. The full scale wave case can then be expected to lie between these and the undisturbed limits. Some areas which will be found unstable by this technique are unlikely to give instability full scale, but the use of the method permits a more reliable comparison of disturbed cases than would otherwise be possible. A disturbance of say 2 degrees magnitude might give the same limits for two hulls, where a larger disturbance will separate them. That there appears to be no simple relationship between a disturbance of given magnitude and a given wave system, does not alter this reasoning, and a small error in the high speed lower limit with disturbance should not prove unduly troublesome.

In all individual model test reports the figures will be to the same scale so that they are directly comparable. Any deviation from, or addition to the techniques of this report, will be particularly noted.

Points arising which need further research include the extension of Gabert and Perring's theory to include the wave case. The first step here would appear to be the answer to the question of why does the model porpoise with a greater undamped amplitude after disturbance in calm water than it does before being disturbed. Having settled this, perhaps a relationship could be established between the frequency of porpoising in waves, the frequency of the calm water disturbed oscillation and the rate of impact of the bow with the wave fronts.

From the discussion on hydrodynamic directional stability it is obvious that some full scale data is necessary to allow an assessment of the scale effect to be made.

The method of plotting stability limits on a draught base needs substantiation, and it could possibly be extended to include the upper limit. At present, only two points are needed to establish a lower limit (as it is a straight line) but more work is necessary before the idea can be fully exploited.

/The

The investigation of the variation of critical trim with mass, moment of inertia and radius of gyration, necessary because of the high beam loadings of these models, is now being carried out and will be reported in Part II of this series.

/LIST OF SYMBOLS

LIST OF SYMBOLS

Load coefficient $C_\Delta = L/wb^3$

Velocity coefficient $C_V = V/\sqrt{gb}$

Longitudinal spray coefficient $C_X = x/b$

Lateral spray coefficient $C_Y = y/b$

Vertical spray coefficient $C_Z = z/b$

L = Load on water - lb.

w = Density of water - lb. per cu. ft.

b = Maximum beam = 0.475 ft.

V = Water speed - ft. per sec.

g = Acceleration due to gravity - 32.2 ft. per sec.^{2}

x = Longitudinal spray co-ordinate - ft.
y = Lateral spray co-ordinate - ft.
z = Vertical spray co-ordinate - ft.
} with step point as origin.

C_L = Total lift coefficient.

C_L' = Tail lift coefficient.

S = Gross mainplane area - sq. ft.

S' = Gross tailplane area - sq. ft.

α = Wing incidence - degrees.

c = S.M.C. = Standard mean chord - ft.

α_K = Keel angle to horizontal - degrees.

η = Elevator angle - degrees.

T_c = Thrust coefficient = $\dfrac{T_o}{\rho V_T^2 d^2}$

T_o = Propeller thrust - lb.

ρ = Density of air - slugs per cu. ft.

V_T = True air speed - ft. per sec.

d = Propeller diameter - ft.

/k_L

LIST OF SYMBOLS
(Contd.)

k_L = Hydrodynamic lift coefficient.

C_β = Deadrise coefficient.

d = Draught - ft.

b_w = Wetted beam - ft.

c = Wetted length of keel - ft.

ρ_w = Density of water - slugs per cu. ft.

$(1-\gamma)c$ = Wetted length of chine - ft.

a_1 = Slope of hydrodynamic lift curve.

S_1 = Projected still water planing area - sq. ft. } without chine immersion.

A_1 = Aspect ratio of S_1.

a_2 = Slope of hydrodynamic lift curve.

S_2 = Projected still water planing area - sq. ft. } with chine immersion.

A_2 = Aspect ratio of S_2.

/LIST OF REFERENCES

LIST OF REFERENCES

No.	Author(s)	Title
1	A. G. Smith J. A. Hamilton	Notes on a detailed research programme on aero and hydrodynamics of hulls with high fineness ratio and full step fairings. M.A.E.E. Report F/Res/221. A.R.C. 13,877. March, 1951.
2	A. G. Smith J. E. Allen	Water and air performance of seaplane hulls as affected by fairing and fineness ratio. R. & M. 2896. August, 1950.
3	T. B. Owen A. G. Kurn A. G. Smith	Model testing technique employed in the R.A.E. seaplane tank. (To be published.)
4	J. M. Benson	The porpoising characteristics of a planing surface representing the fore-body of a flying boat hull. S.471 (6166), NACA/ARR (WR L - 479). October, 1942.
5	D. M. Ridland	A comparison of three types of chine strip for use on models for test in the seaplane towing tank. M.A.E.E. Tech. Memo. 17. November, 1952.
6	R. Parker	Notes on a research aircraft proposed for use as a seaplane test vehicle for the development of advanced designs and basic research work. M.A.E.E. Report F/Res/229. A.R.C. 15,538. December, 1952.
7	F. W. S. Locke	A method for making quantitative studies of the main spray characteristics of flying-boat-hull models. NACA/ARR/3K11. November, 1943.
8	K. W. Clarke W. D. Tye	Some measurements of ground effect in the seaplane tank. R.A.E. Report B.A. 1421. Aero. Tech. 1324. A.R.C. 3263. September, 1937.
9	A. G. Smith H. G. White	A review of porpoising instability of seaplanes. R. & M. 2852. February, 1944.
10	W. G. A. Perring H. Glauert	The stability on the water of a seaplane in the planing condition. R. & M. 1493. September, 1932.
11	K. S. M. Davidson F. W. S. Locke A. Suarez	Porpoising. A comparison of theory with experiment. NACA/ARR/3G07. July, 1943.
12	A. G. Smith	Notes on the water flow over a wedge. M.A.E.E. Tech. Memo. 18. A.R.C. 15,934. March, 1953.
13	L. P. Coombes W. G. A. Perring L. Johnston	The use of dynamically similar models for determining the porpoising characteristics of seaplanes. R. & M. 1718. November, 1935.

/14

LIST OF REFERENCES (Contd.)

No.	Author	Title
14	J. P. Gott	Note on the technique of tank testing dynamic models of flying boats as affected by recent full scale experience. A.R.C. 4378. December, 1939.
15	G. L. Fletcher	Tank tests on a jet propelled boat seaplane fighter (Saunders-Roe E6/44). R. & M. 2718. January, 1946.
16	F. W. S. Locke W. C. Hugli	A method for studying the longitudinal dynamic stability of flying-boat-hull models at high planing speeds and during landing. NACA/ARR/4H31. April, 1945.
17	C. H. E. Warren W. D. Tye	Calibration of the wavemaker in the R.A.E. towing tank. R.A.E. Tech. Note Aero. 1764. A.R.C. 9770. March, 1946.
18	F. R. J. Spearman	Measurement of dynamic performance of desynn repeater. R.A.E. Tech. Note Instn. 122. August, 1948.
19	T. B. Owen	Model tests on the directional stability on the water of the Princess flying boat. R.A.E. Tech. Memo Aero. 262. April, 1952.
20	F. W. S. Locke	A graphical method for interpolation of hydrodynamic characteristics of specific flying boats from collapsed results of general tests of flying-boat-hull models. NACA/TN/1259. January, 1948.
21	D. Whittley P. Crewe	An interim report on the generalised presentation of tank tests on a seaplane hull or float. Saunders-Roe Report No. AH/37/T. March, 1947.
22	W. G. A. Perring L. Johnston	Hydrodynamic forces and moments on a simple planing surface and on a flying boat hull. R. & M. 1646. February, 1935.
23	R. E. Olson N. S. Land	Methods used in the N.A.C.A. tank for the investigation of the longitudinal stability characteristics of models of flying boats. NACA Report 753. 1943.
24	F. W. S. Locke	"General" main-spray tests of flying-boat models in the displacement range. NACA/ARR/5A02. April, 1945.
25	E. P. Warner	Airplane design - performance. Mcgraw-Hill Book Co., Inc., New York and London.

/APPENDIX I

APPENDIX I

MODEL HULL DESIGN

1. GENERAL

In the basic design reference is made to a streamline shape. This is defined[25] by

forward 40%: $\left(\frac{x}{L}\right)^2 + 0.16y^2 = 0.16$ .....(1)

aft 60%: $\left(\frac{x}{L}\right)^2 + 0.0679y^2 + 0.292ly = 0.36$ .....(2)

where y = diameter at x,

x = distance from point of maximum diameter, and

L = overall length of streamline shape.

The maximum hull beam, b = 0.475 feet, maximum height = 2b and step depth = 0.15b.

2. FOREBODY

The forebody is 6b long and is of constant beam for 3b forward of the step. The beam for any station in the forward half is given by equation (1). The tumble home is semi-circular in cross-section with the beam at that section as diameter. Forebody warp varies from model to model, but in the case of zero warp, deadrise is constant at 25° for the first half of the forebody forward of the step and increases in a manner giving good lines to 63° at the forward perpendicular. In side view the forebody keel is parallel to the hull crown for the first 3b forward of the step, it is then elliptical, rising to 1b above the keel line at the forward perpendicular. All forebody cross-sections are parallel sided.

3. AFTERBODY

Afterbody length and angle varies to conform to Table I, but the plan view of the afterbody planing bottom is defined by equation (2). Afterbody deadrise is 26° at the main step, increasing to 30° in 40% of afterbody length and remaining constant at 30° to the aft step. Cross-sections are parallel sided up to at least the height of the aft step, but above this a fairing was added to carry the tail unit. This was drawn so as to give good lines and can be seen in Figure 3. The hull crown aft of the main step is parallel to the forebody keel and the afterbody tumble home is semi-circular in cross-section. The aerodynamic tail arm is constant, so whether or not there is a counter, and if so its design, is dependent on afterbody length and angle.

/ TABLE I

TABLE I

Models for hydrodynamic stability tests

Model	Forebody warp	Afterbody length	Afterbody-forebody keel angle	Stop form	To determine effect of
	degrees per beam	beams	degrees		
A	0	5	6	Unfaired transverse. Step depth 0.15 beam.	Forebody warp
B	4	5	6		
C	8	5	6		
D	0	4	6		Afterbody length
A	0	5	6		
E	0	7	6		
F	0	9	6		
G	0	5	4		Afterbody angle
A	0	5	6		
H	0	5	8		

/ TABLE II

TABLE II

Model Aerodynamic data

Mainplane	
Section	Gottingen 436 (mod.)
Gross area	6.85 sq. ft.
Span	6.27 ft.
S.M.C.	1.09 ft.
Aspect ratio	5.75
Dihedral (on 30% spar axis)	3° 0'
Sweepback (on 30% spar axis)	4° 0'
Wing setting (root chord to hull datum)	6° 9'
Tailplane	
Section	R.A.F. 30 (mod.)
Gross area	1.33 sq. ft.
Span	2.16 ft.
Total elevator area	0.72 sq. ft.
Tailplane setting (root chord to hull datum)	2° 0'
Fin	
Section	R.A.F. 30
Gross area	0.80 sq. ft.
Height	1.14 ft.
General	
* C.G. position	
distance forward of step point	0.237 ft.
distance above step point	0.731 ft.
* ¼ chord point S.M.C.	
distance forward of step point	0.277 ft.
distance above step point	1.015 ft.
* Tail arm l (C.G. to hinge axis)	3.1 ft.
* Height of tailplane root chord L.E. above hull crown	0.72 ft.

* These distances are measured either parallel to or normal to the hull datum.

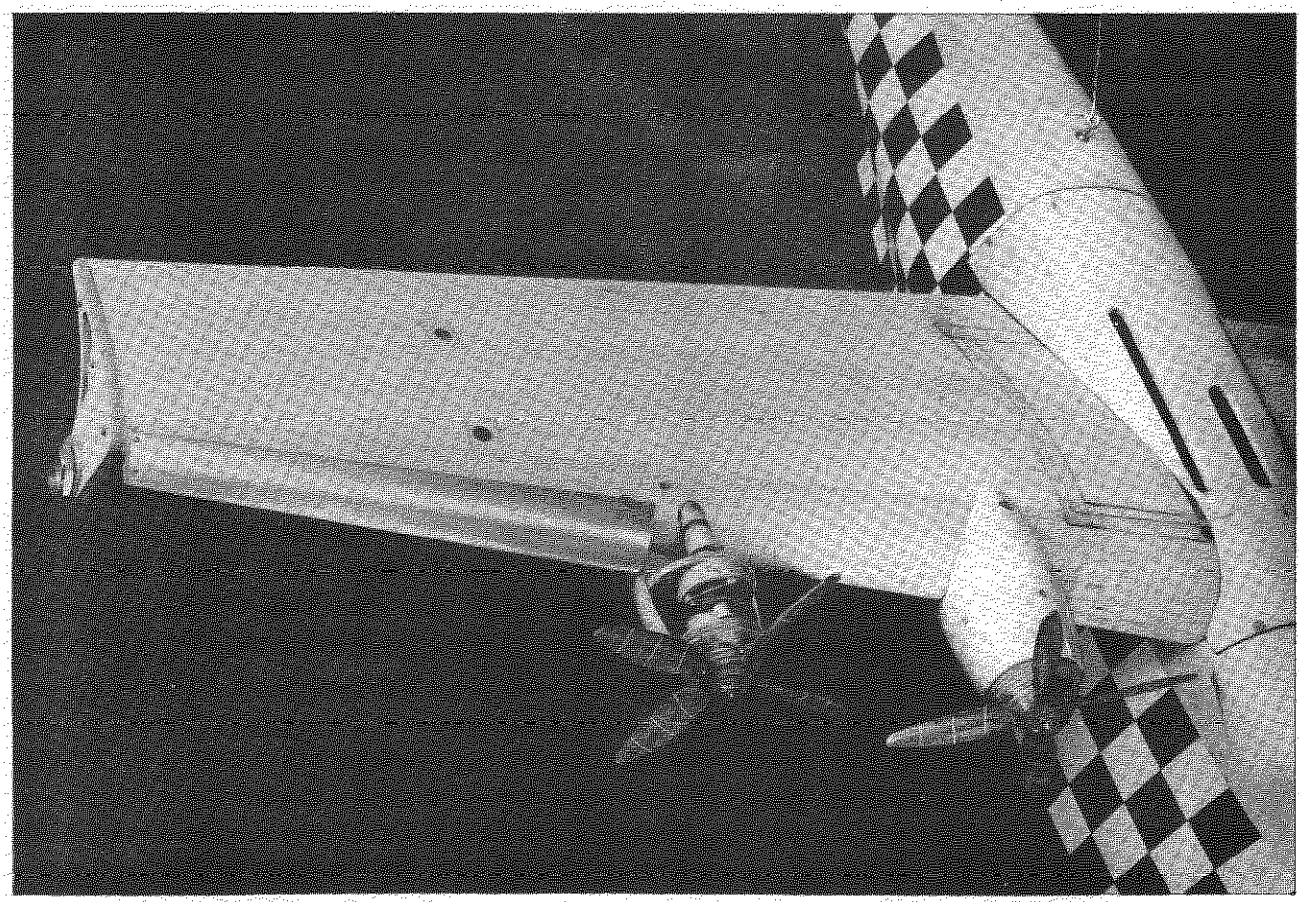

FIG.1. MODEL WING WITH TURBINES

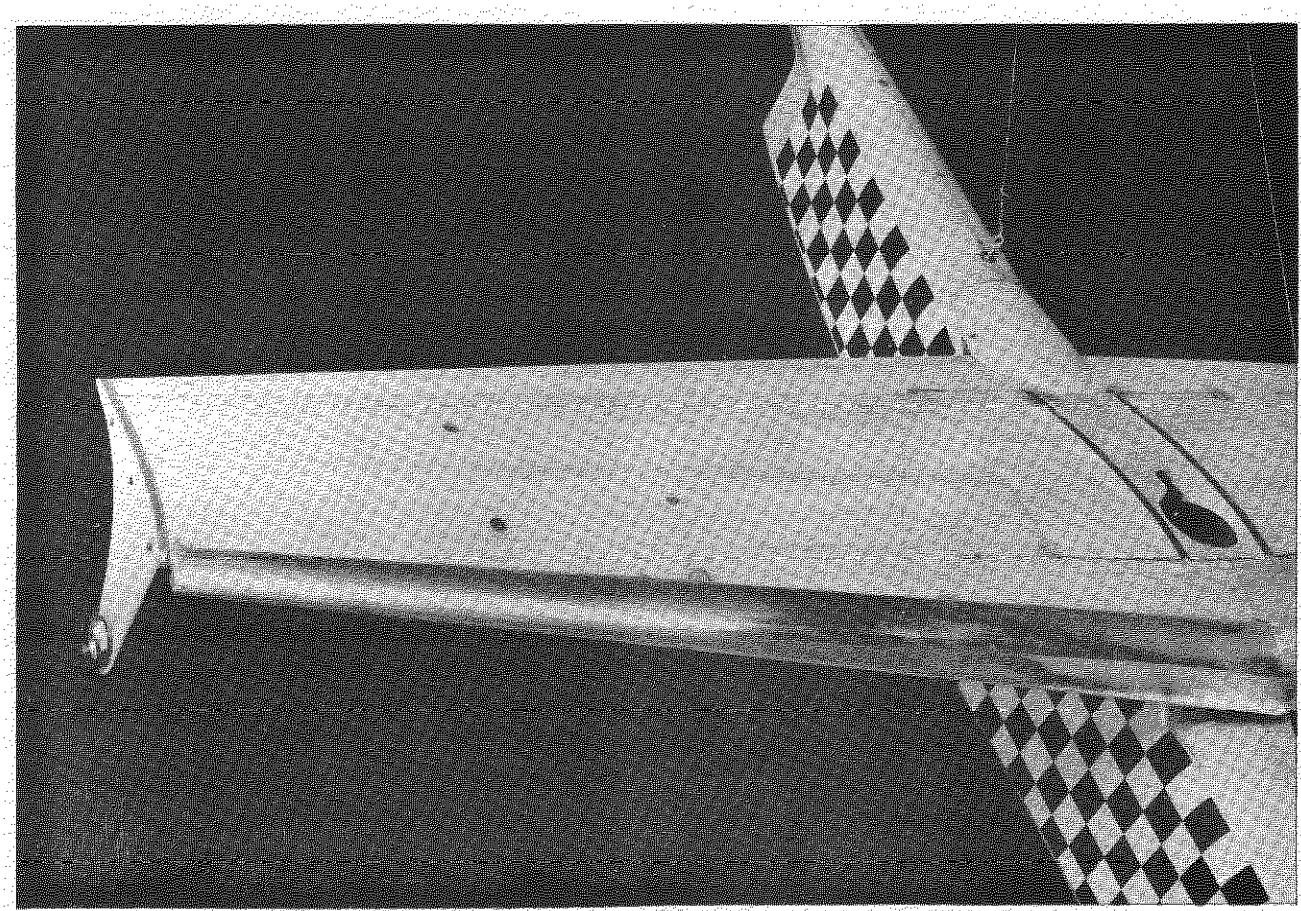

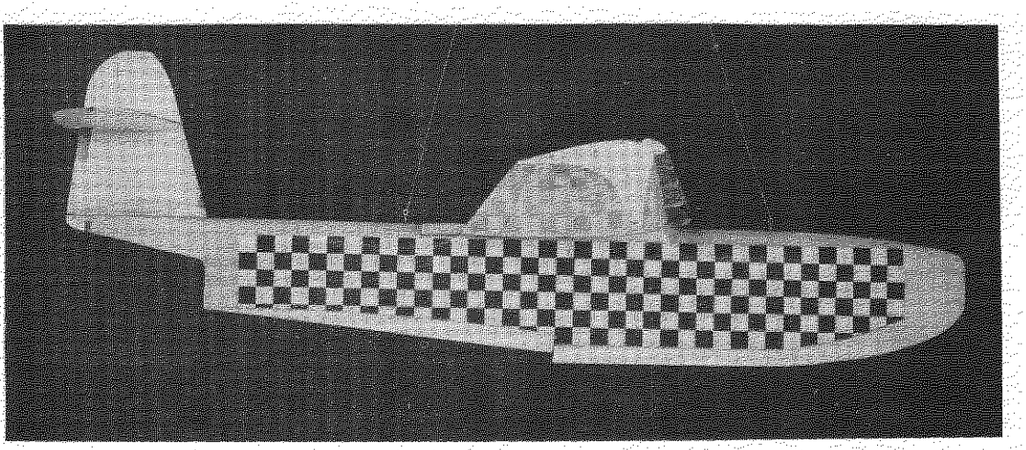

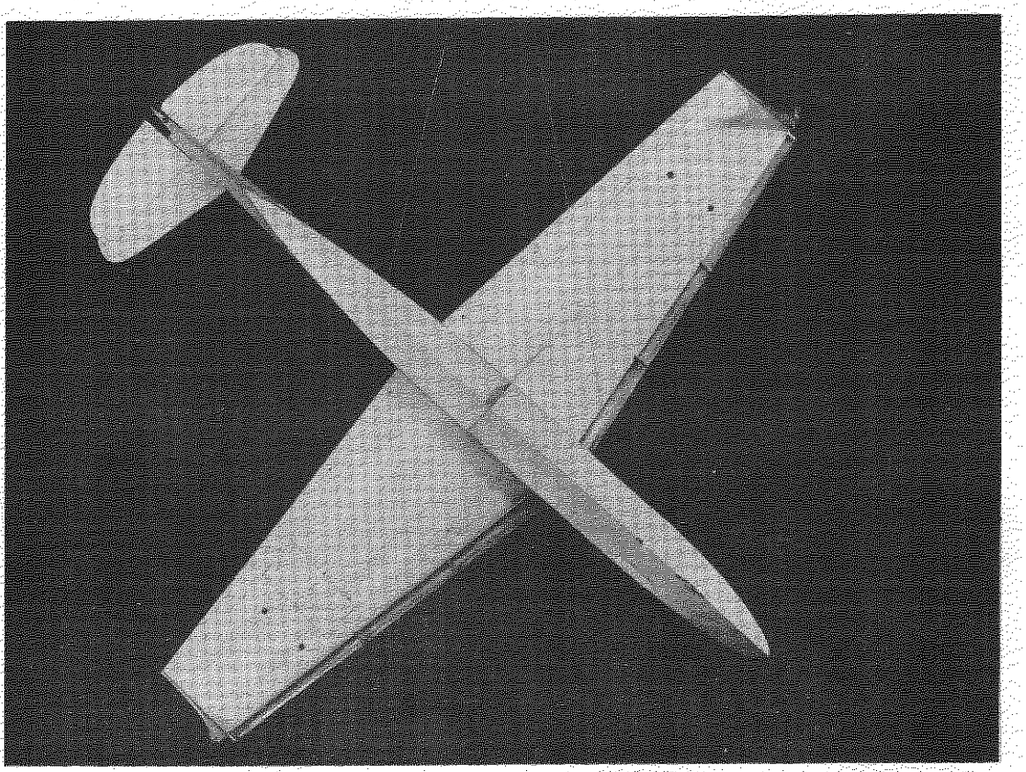

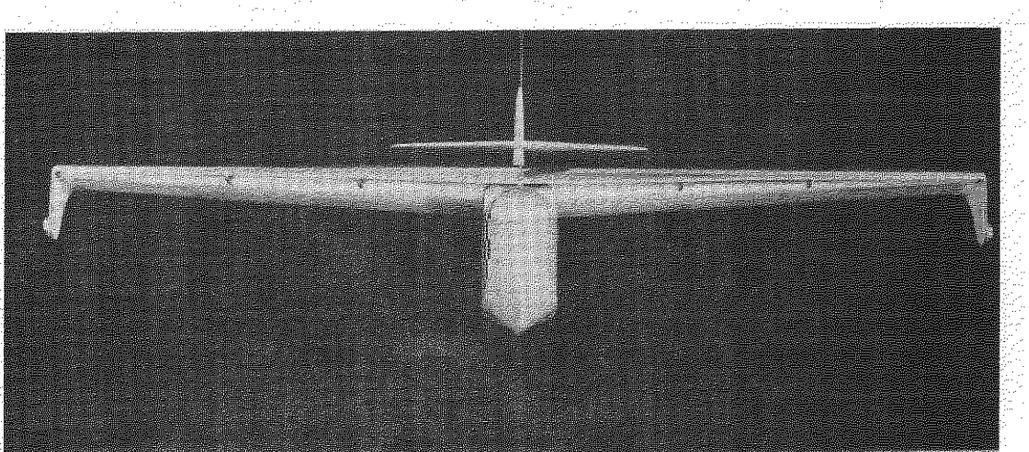

FIG.3. PHOTOGRAPHS OF BASIC MODEL. (MODEL A)

FIG.4.

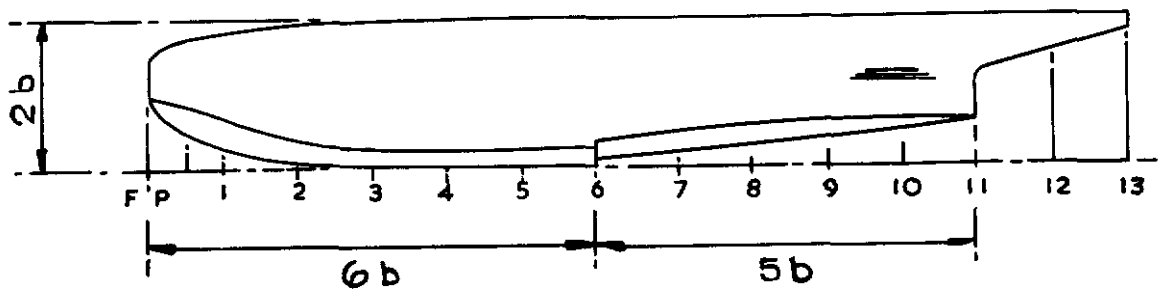

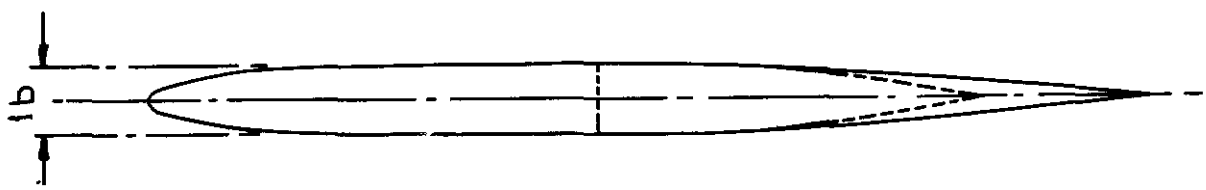

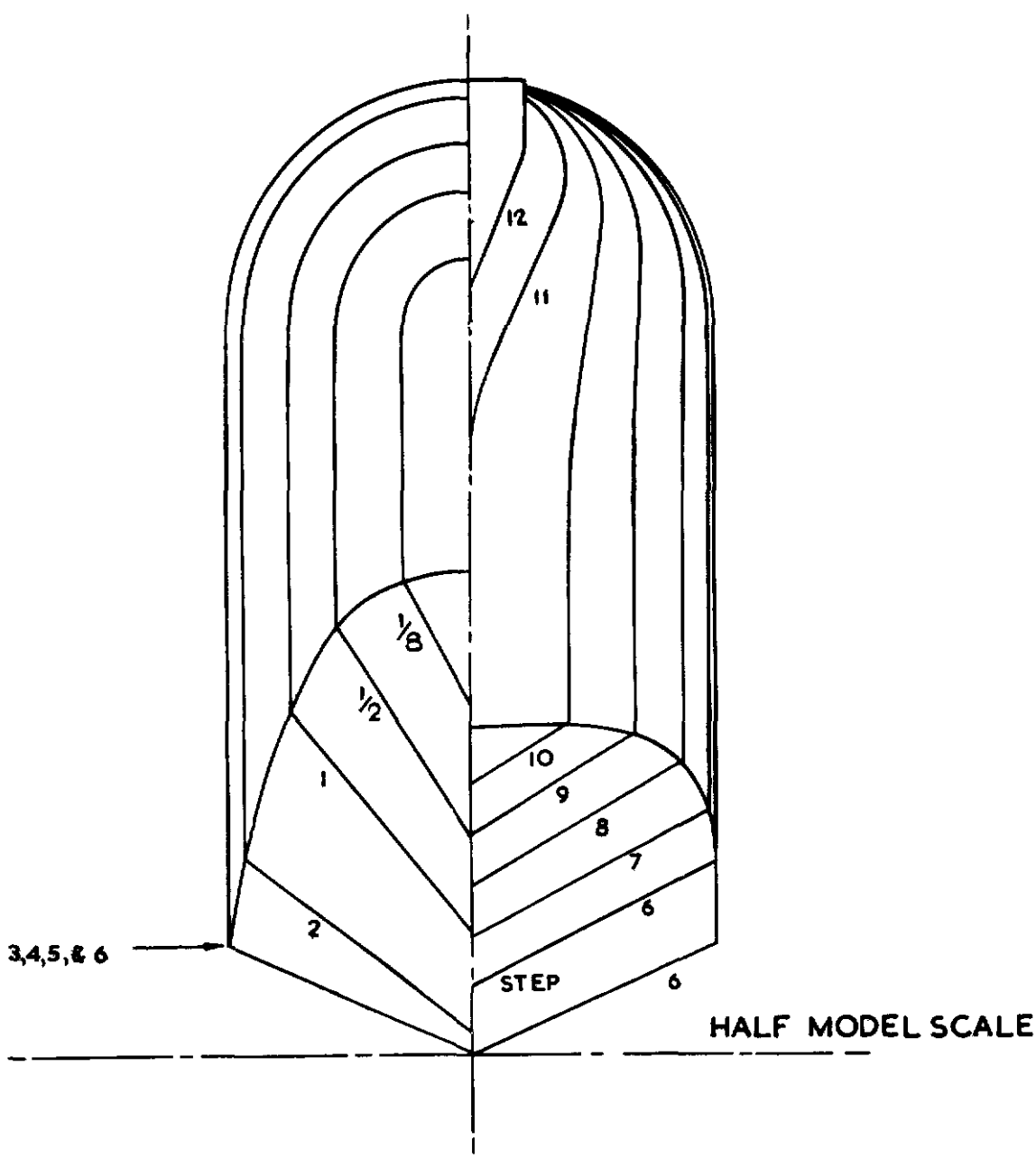

MODEL A

HULL LINES

FIG 5

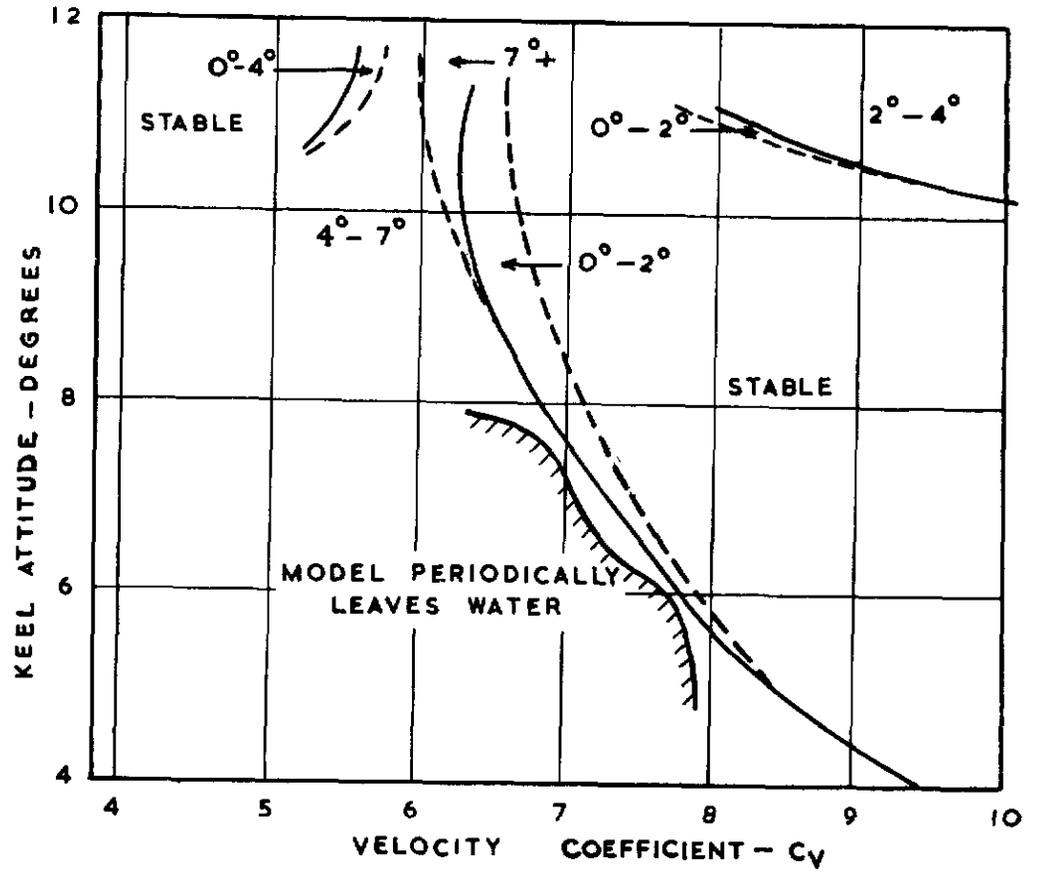

(A) UNDISTURBED CASE

FIGURES INDICATE
AMPLITUDES OF
PORPOISING IN DEGREES

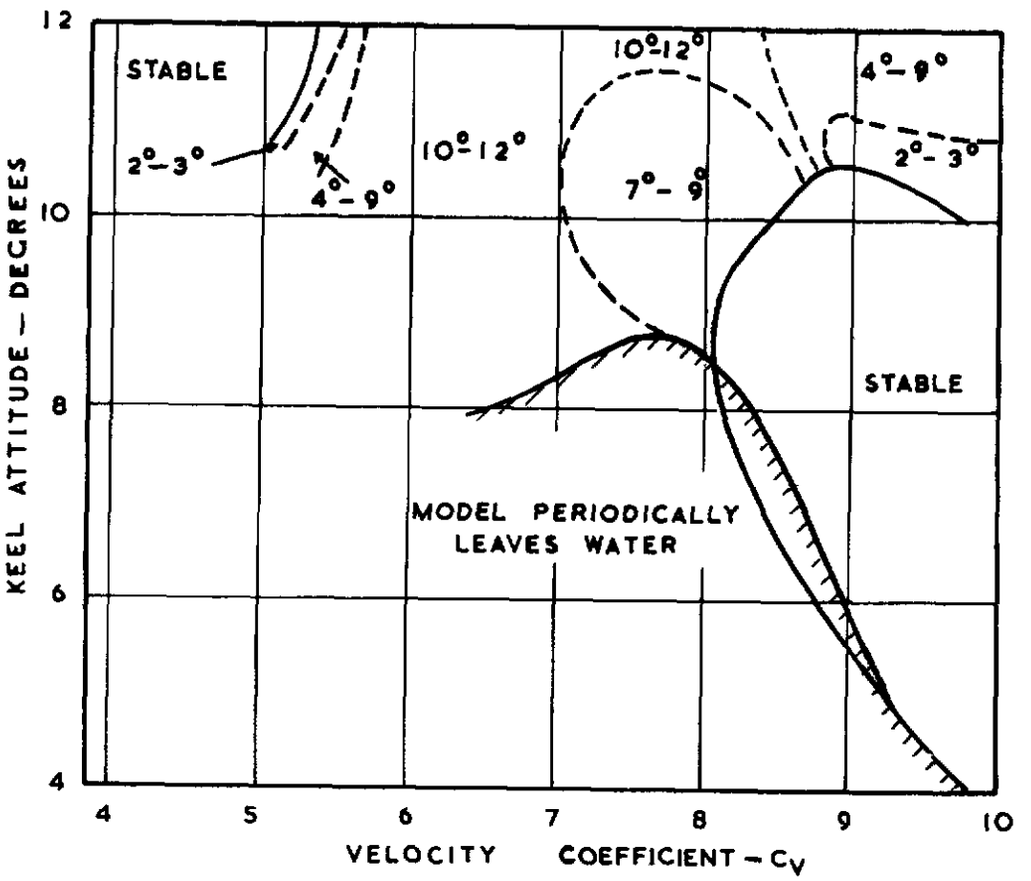

(B) WITH 5° NOSE DOWN DISTURBANCE

MODEL A

DIVISION OF UNSTABLE REGION INTO REGIONS
OF EQUAL STEADY OSCILLATIONS

FIG 6

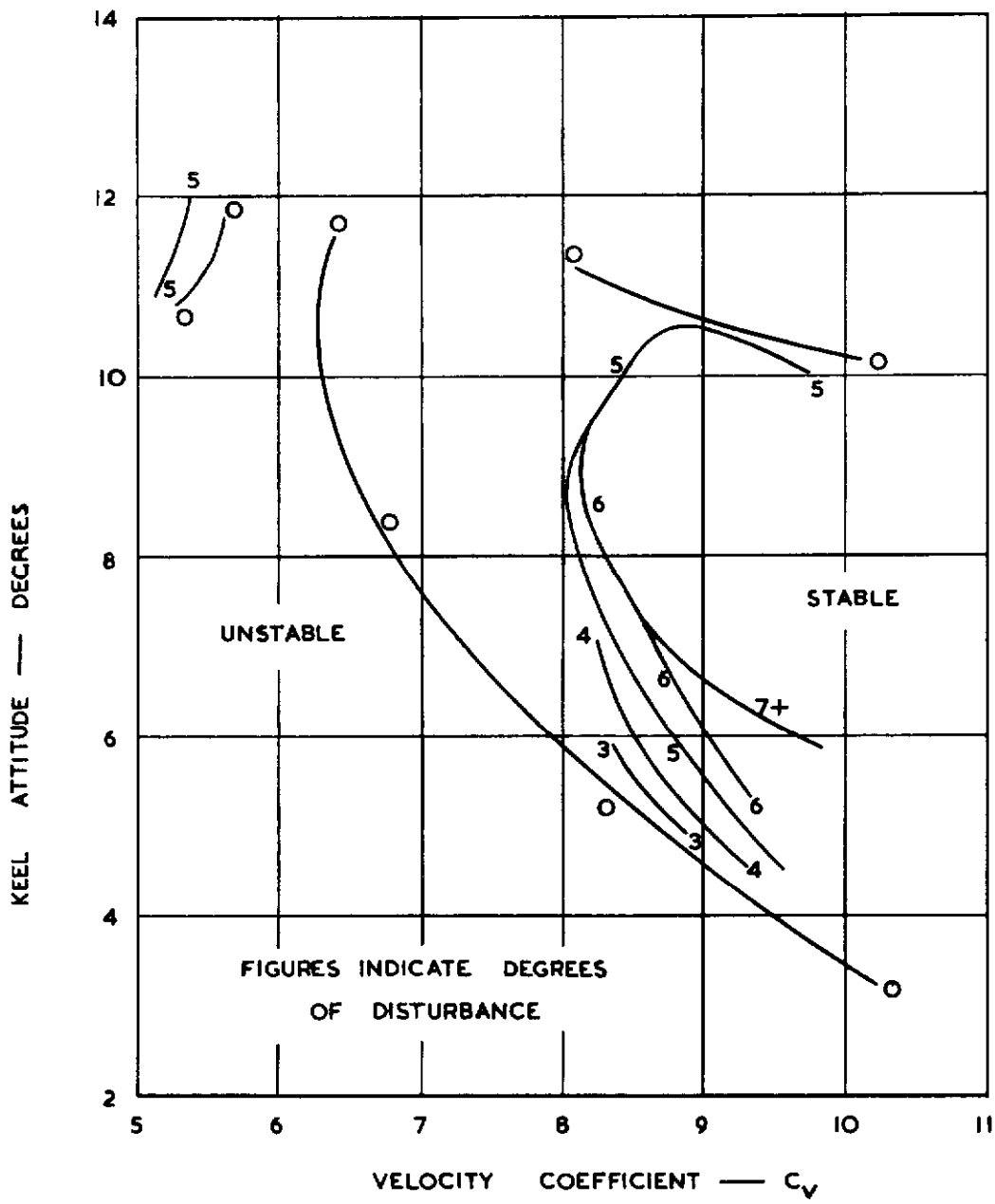

MODEL A

LONGITUDINAL STABILITY LIMITS FOR

0,3,4,5,6 AND 7 DEGREES OF DISTURBANCE

FIG 7A

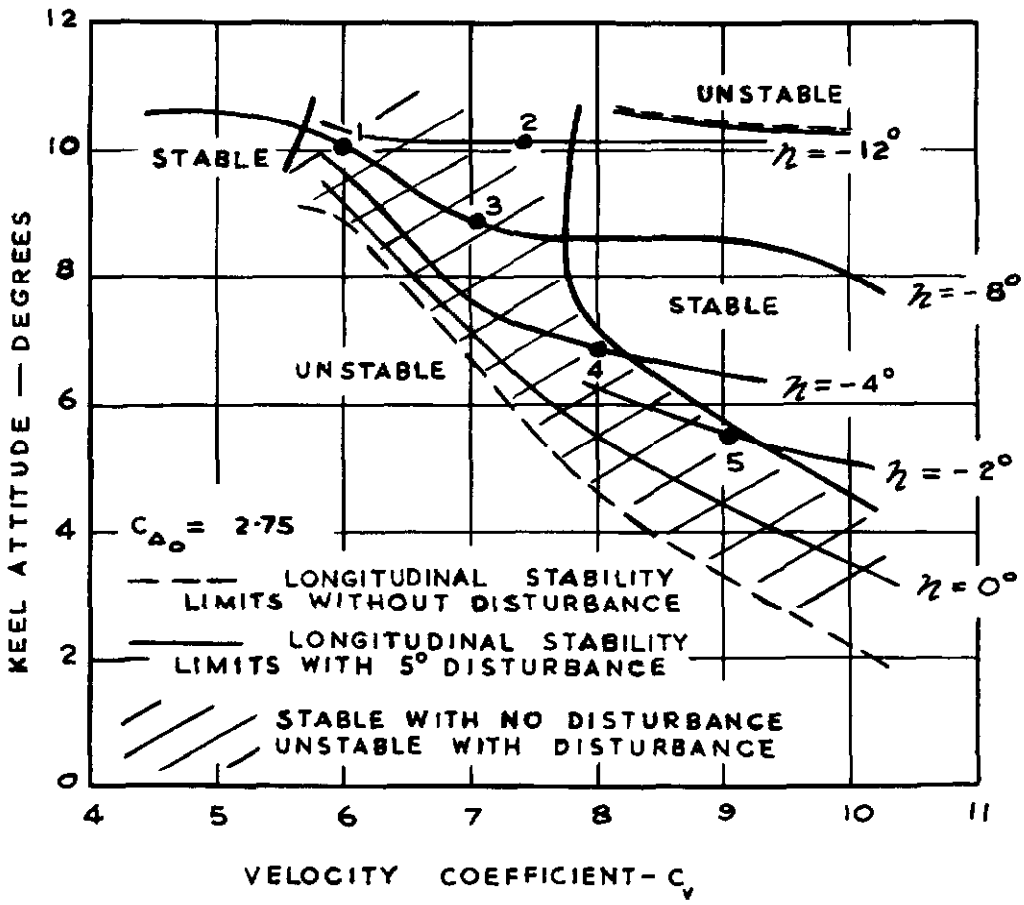

CASE NO	V FT.PER SEC	C_V	η DEGS	α_K DEGS	CRITICAL DISTURBANCE DEGREES	$\frac{\sqrt{C_\Delta}}{C_V}$
1	23·5	6·00	− 8	10·1	4·0	0·23
2	29·0	7·42	− 12	10·1	4·5	0·16
3	27·5	7·04	− 8	8·9	3·0	0·18
4	31·5	8·06	− 4	6·8	3·0	0·15
5	35·5	9·07	− 2	5·4	3·5	0·13

MODEL B

(A) POINTS INVESTIGATED

WAVE — DISTURBANCE CORRELATION

FIG 7B

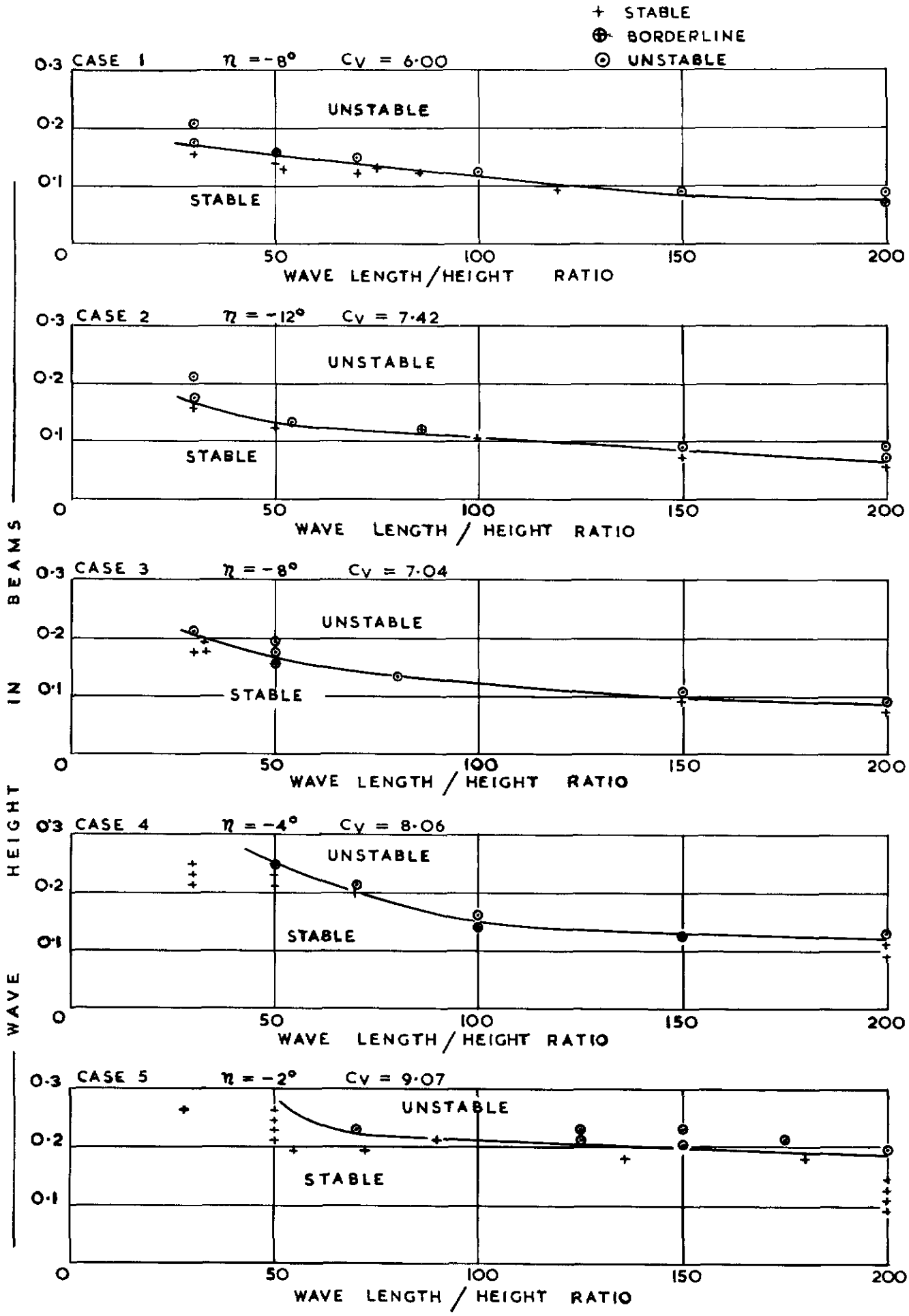

MODEL B

(B) WAVE HEIGHTS NECESSARY TO INDUCE INSTABILITY

WAVE — DISTURBANCE CORRELATION

FIG 8

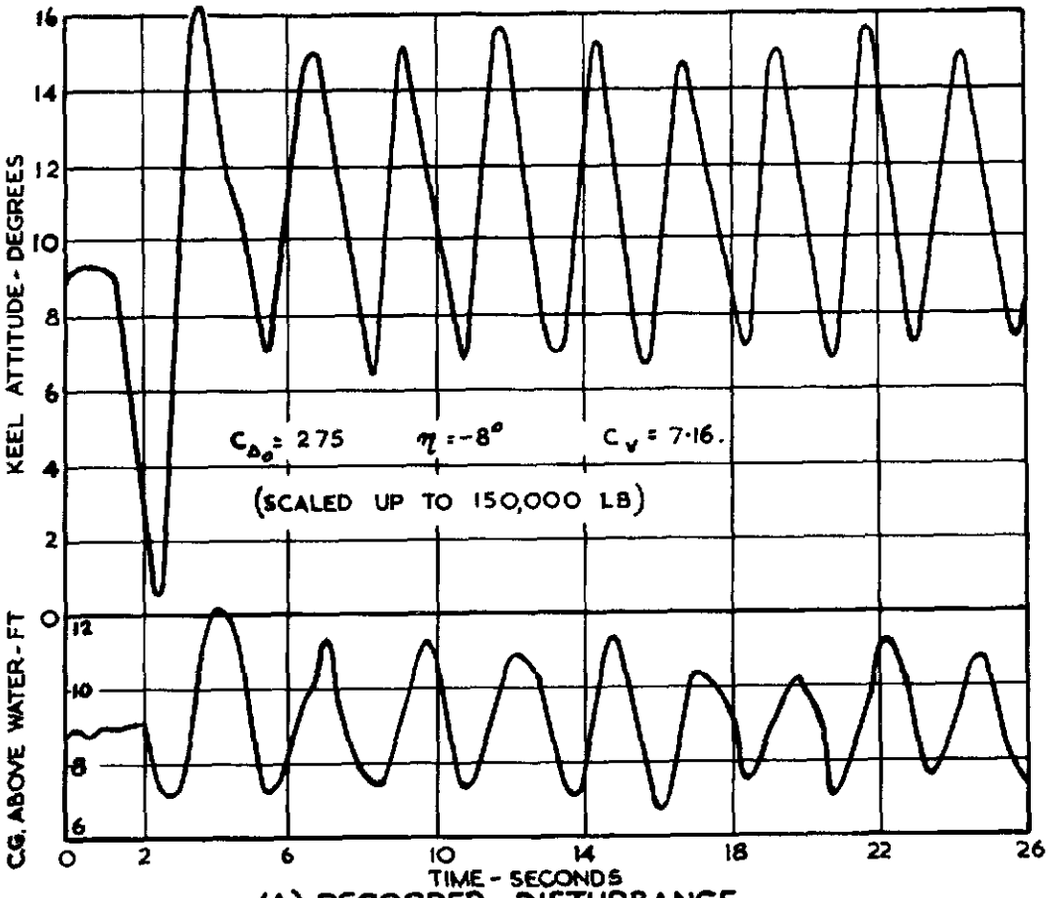

(A) RECORDED DISTURBANCE

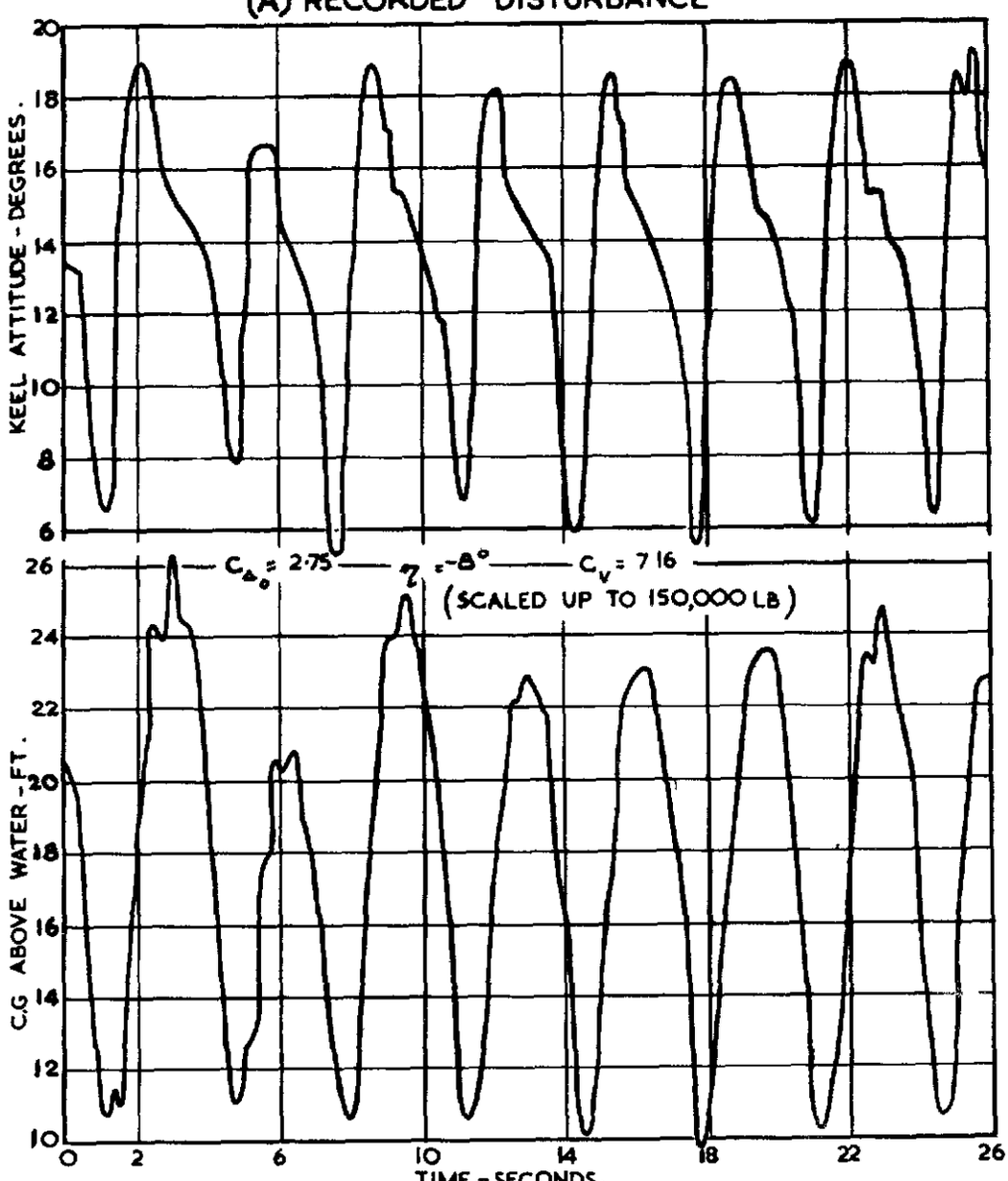

(B) RECORDED STEADY SPEED RUN THROUGH WAVES
(WAVE LENGTH / HT RATIO: 110 · 1 WAVE HT = 2·35 FT.)

MODEL A - RECORDINGS FROM LONGITUDINAL STABILITY RIG ATTACHMENTS.

MODEL A

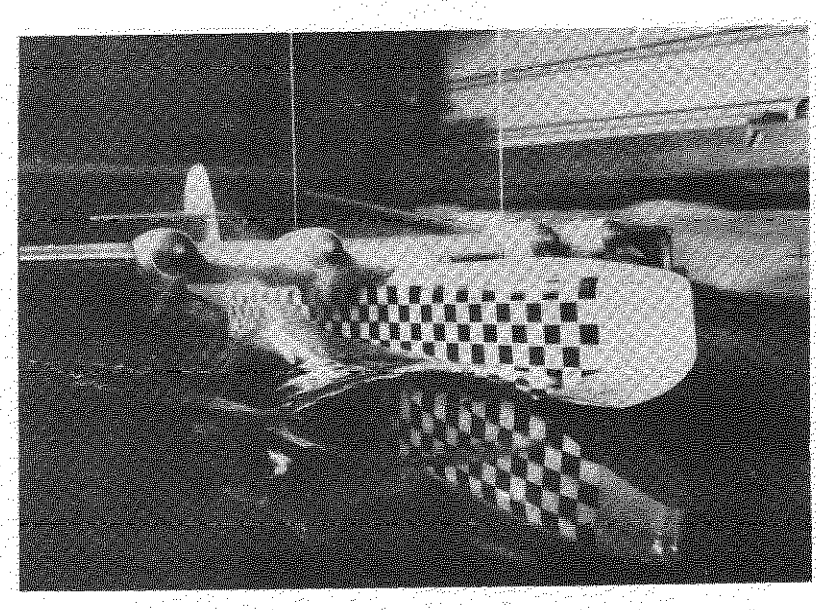

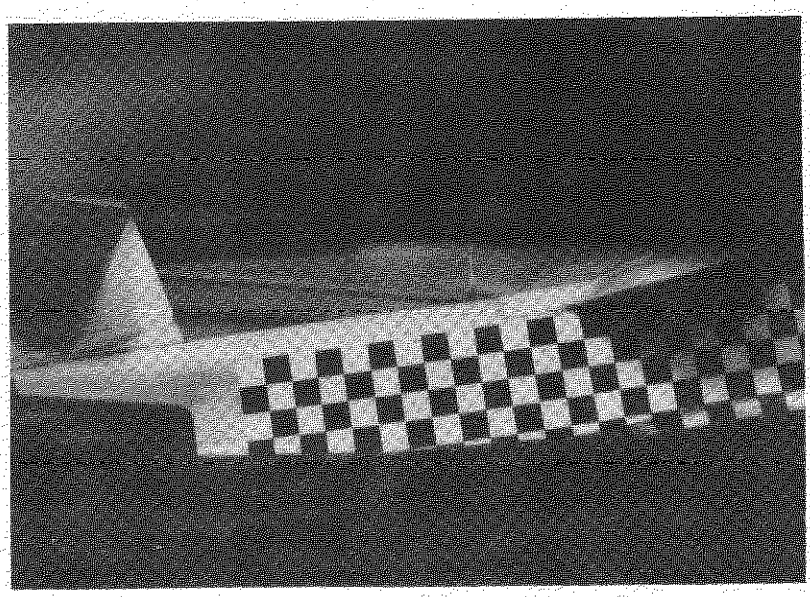

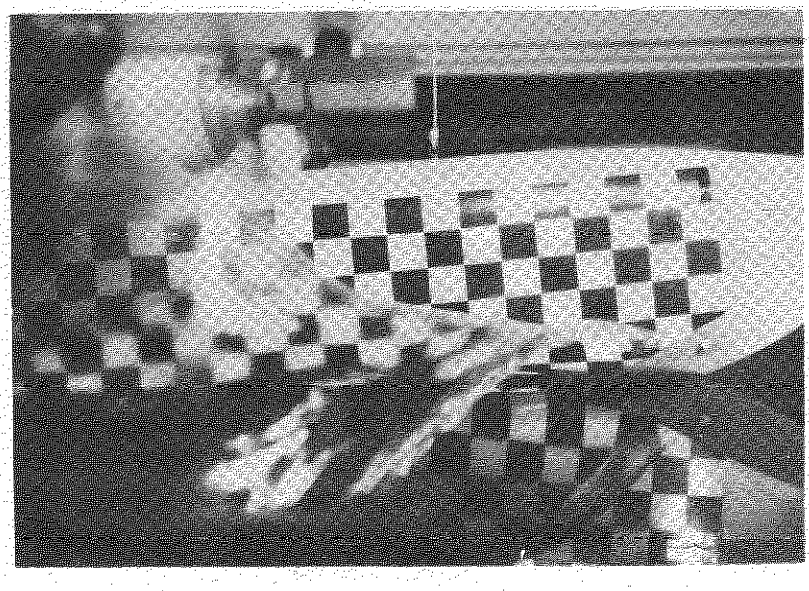

FIG.9. SPRAY PHOTOGRAPHS AT $C_y = 2.07.C_{\Delta p} = 2.75$

FIG 10

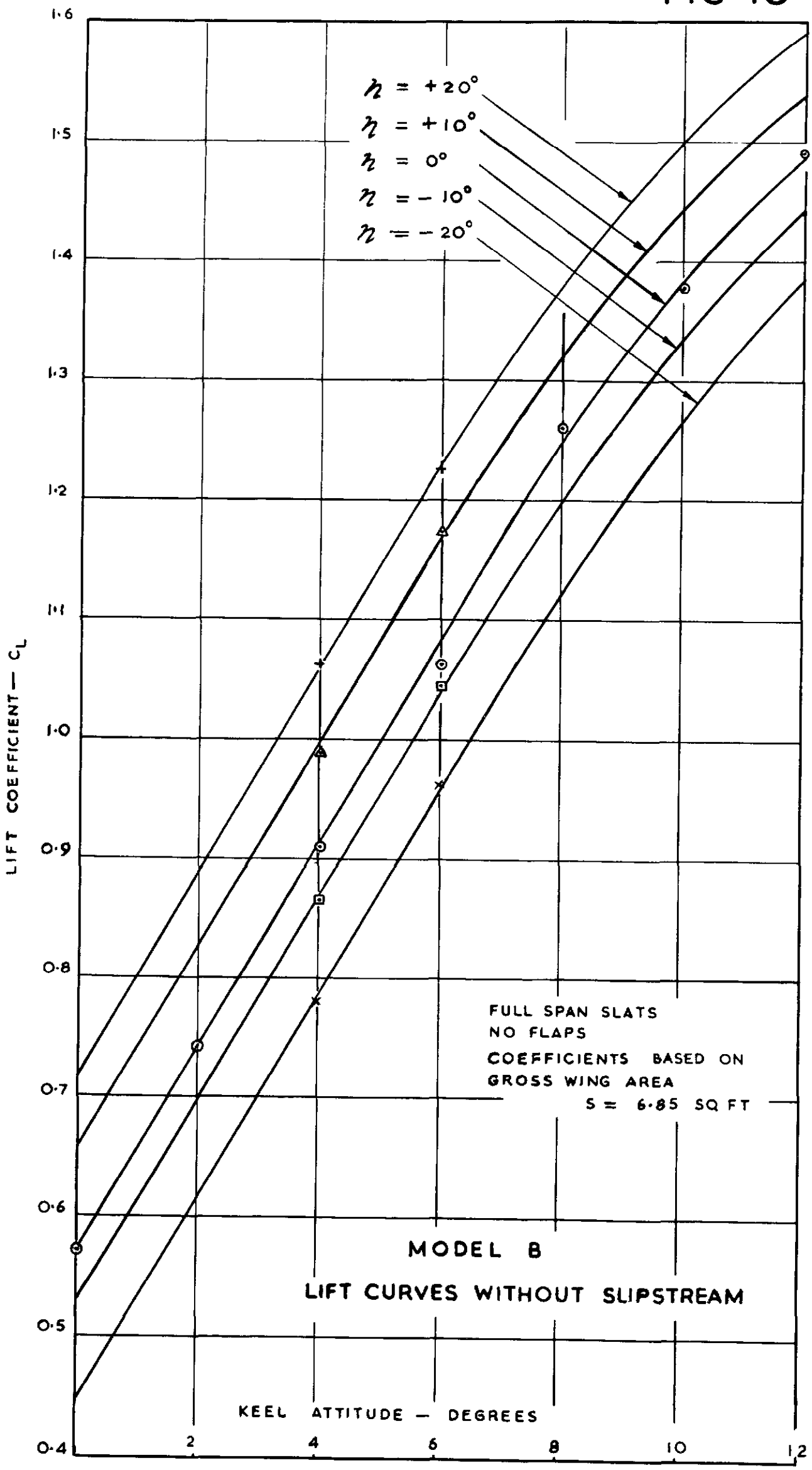
η = +20°
η = +10°
η = 0°
η = −10°
η = −20°
LIFT COEFFICIENT — C_L
1·6
1·5
1·4
1·3
1·2
1·1
1·0
0·9
0·8
0·7
0·6
0·5
0·4
2
4
6
8
10
12
KEEL ATTITUDE — DEGREES
FULL SPAN SLATS
NO FLAPS
COEFFICIENTS BASED ON
GROSS WING AREA
S = 6·85 SQ FT
MODEL B
LIFT CURVES WITHOUT SLIPSTREAM

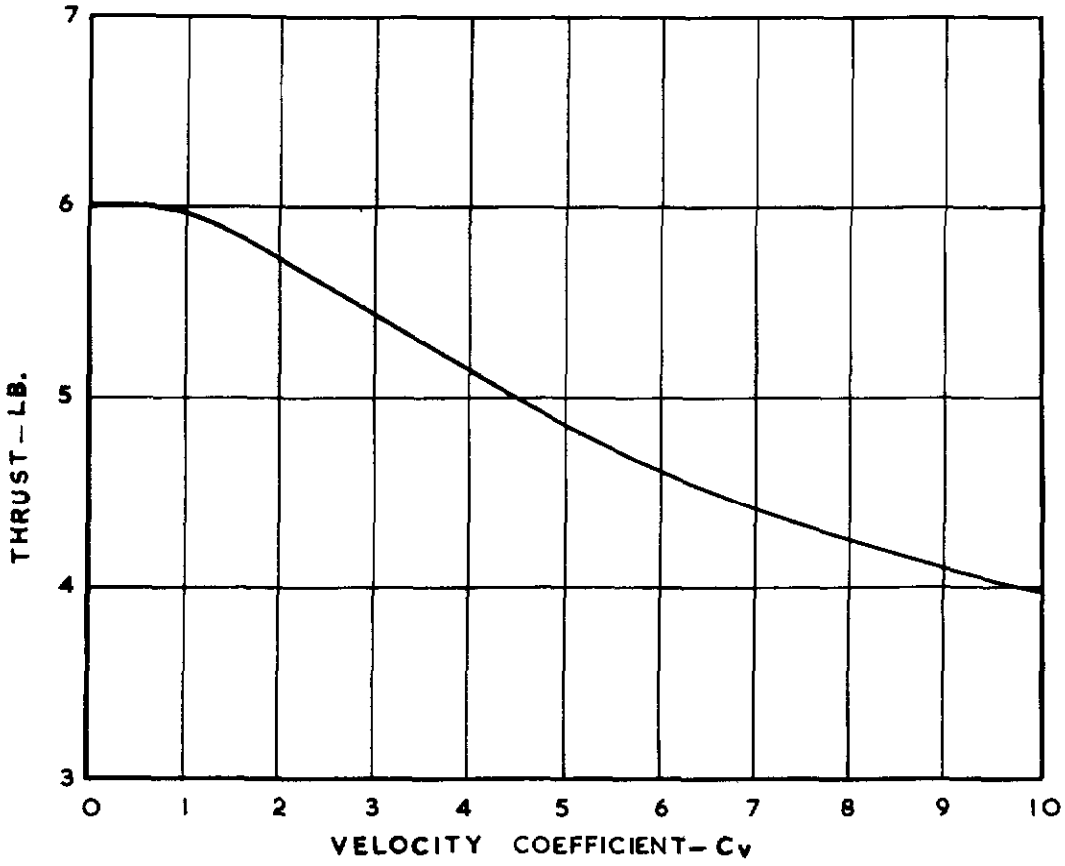

FIG. 11. MODEL THRUST AGAINST VELOCITY COEFFICIENT

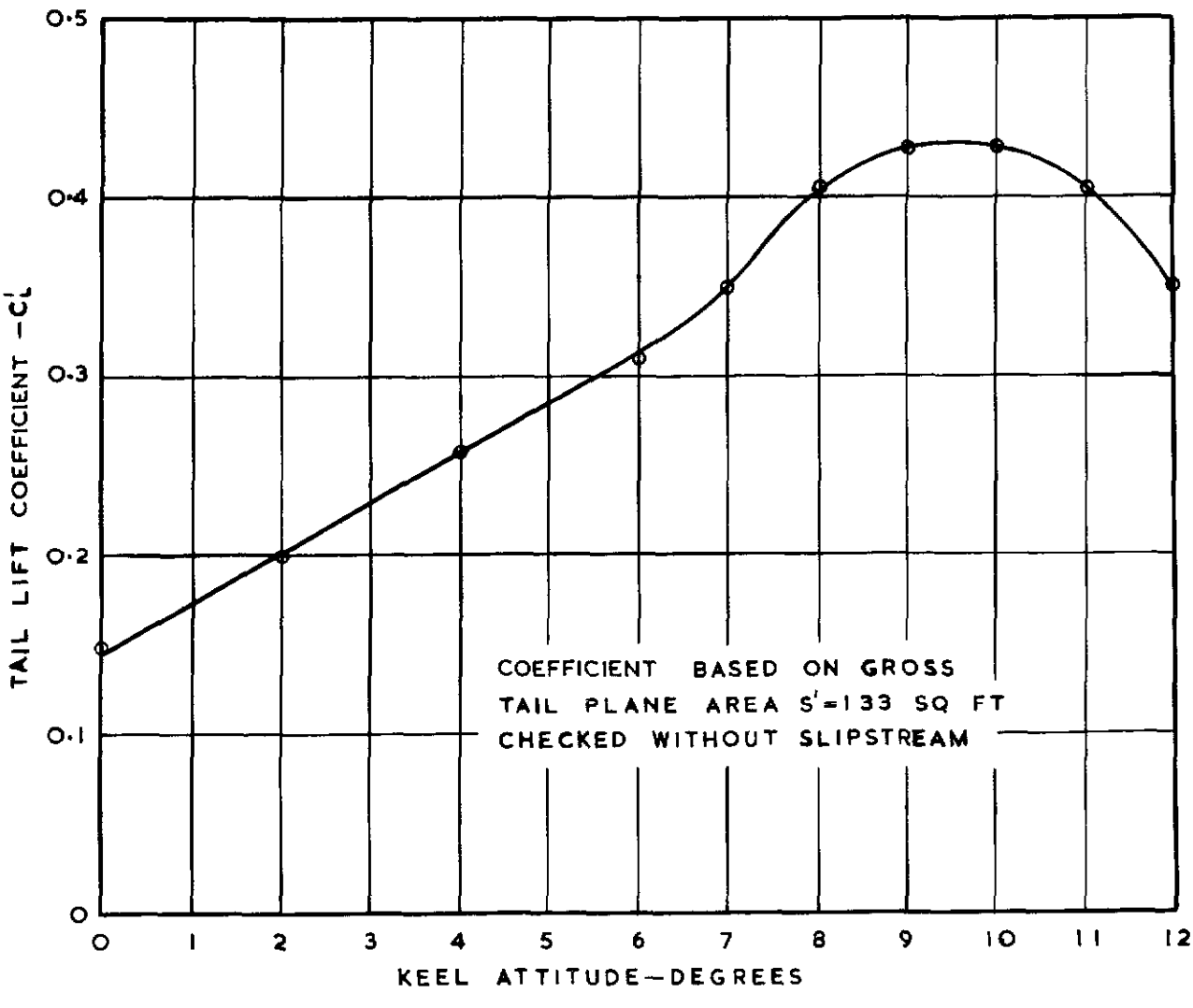

FIG. 12. TAIL PLANE LIFT CURVE

FIG 13

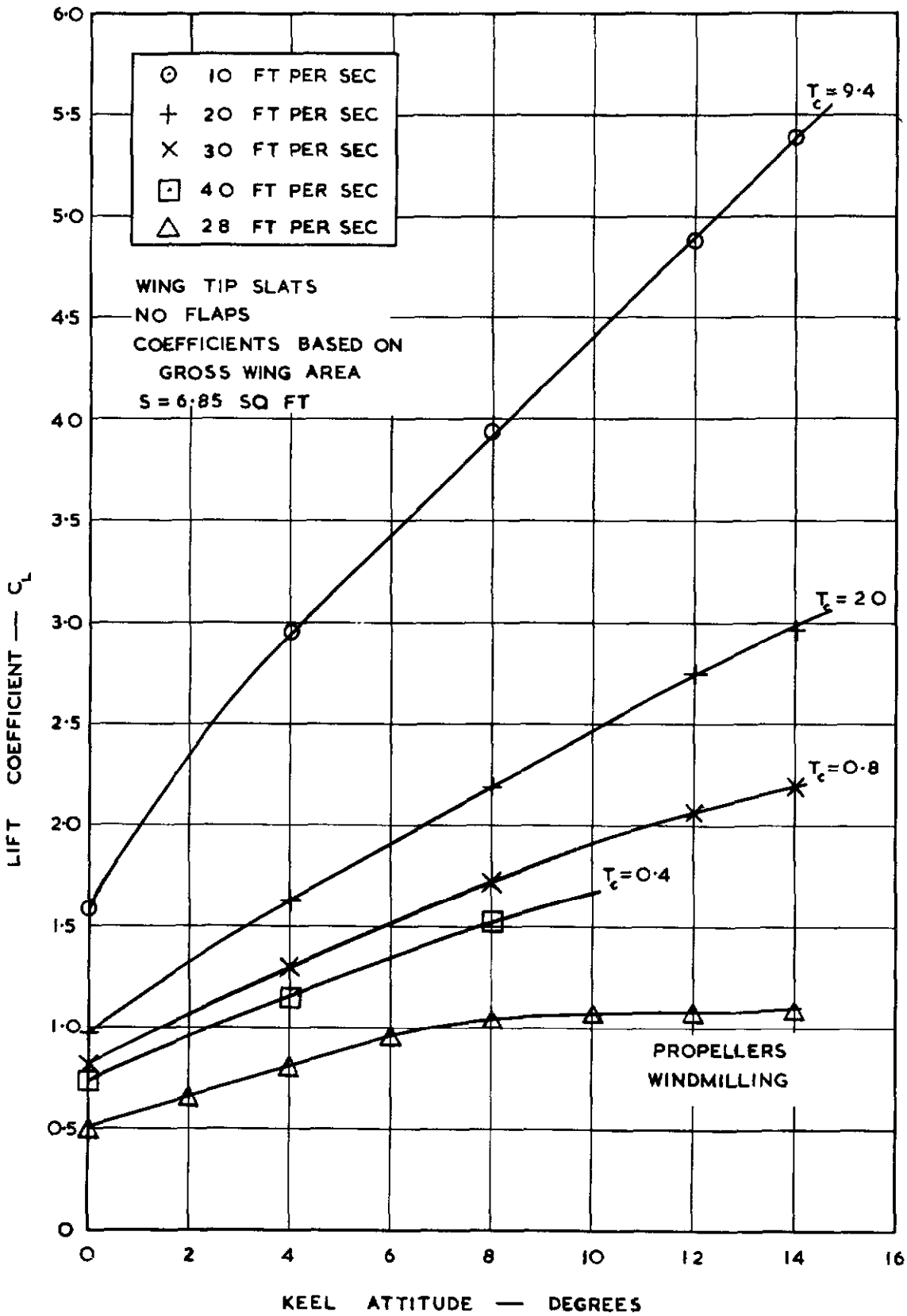

MODEL B

LIFT CURVES WITH SLIPSTREAM

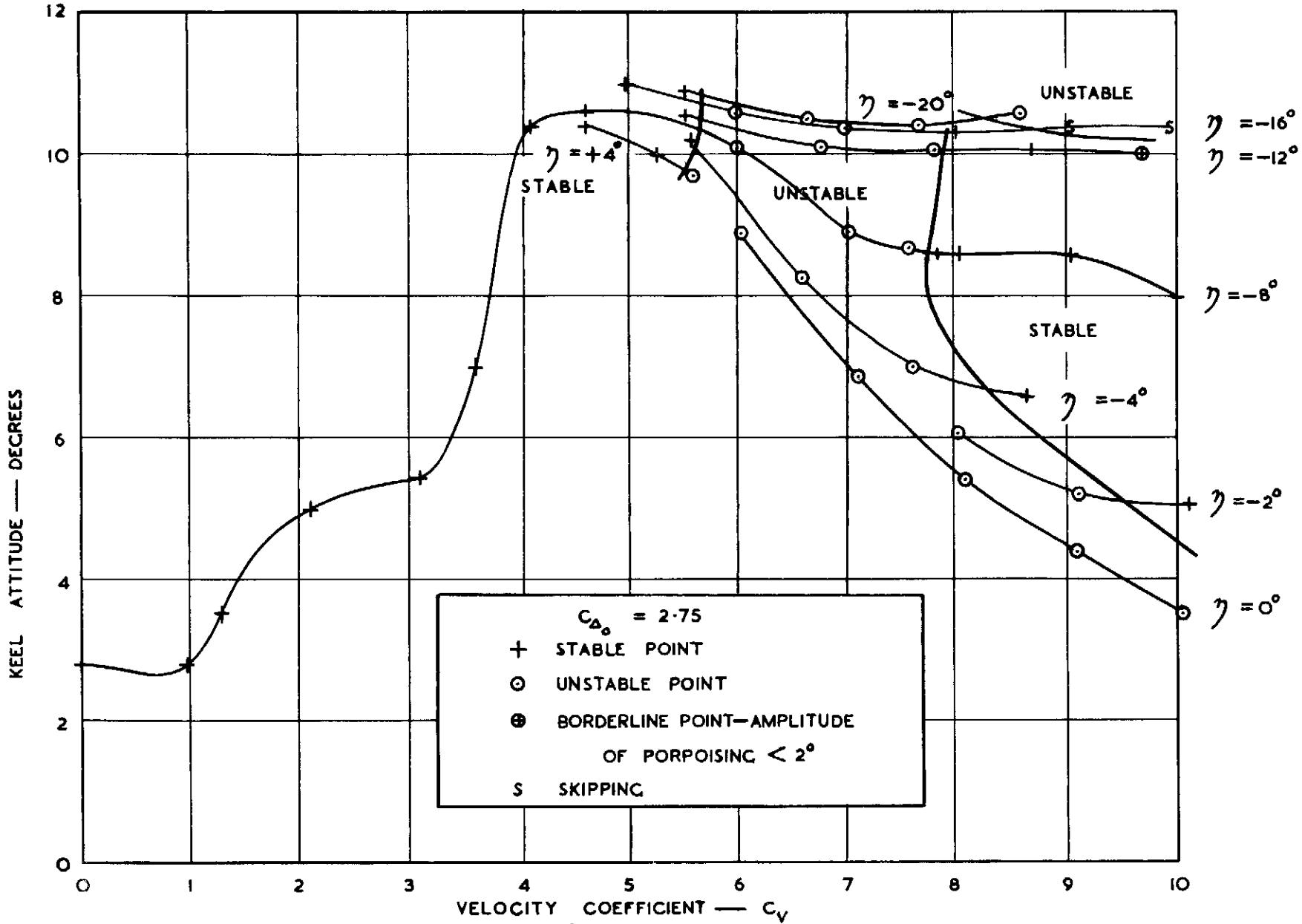

MODEL B

LONGITUDINAL STABILITY DIAGRAM WITH 5° NOSE-DOWN DISTURBANCE

FIG 14

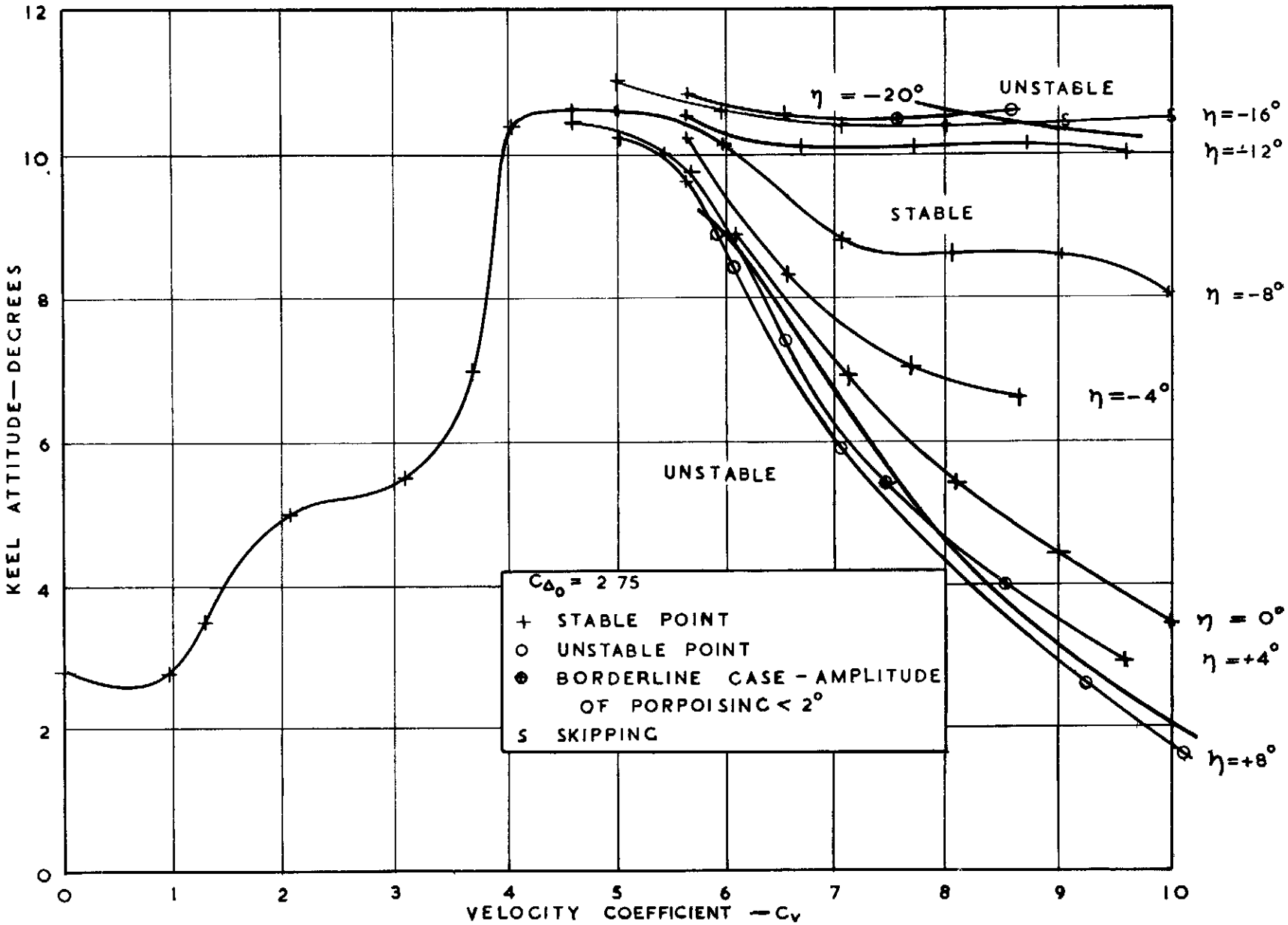

MODEL B
LONGITUDINAL STABILITY DIAGRAM WITHOUT DISTURBANCE

FIG 15

FIG 16

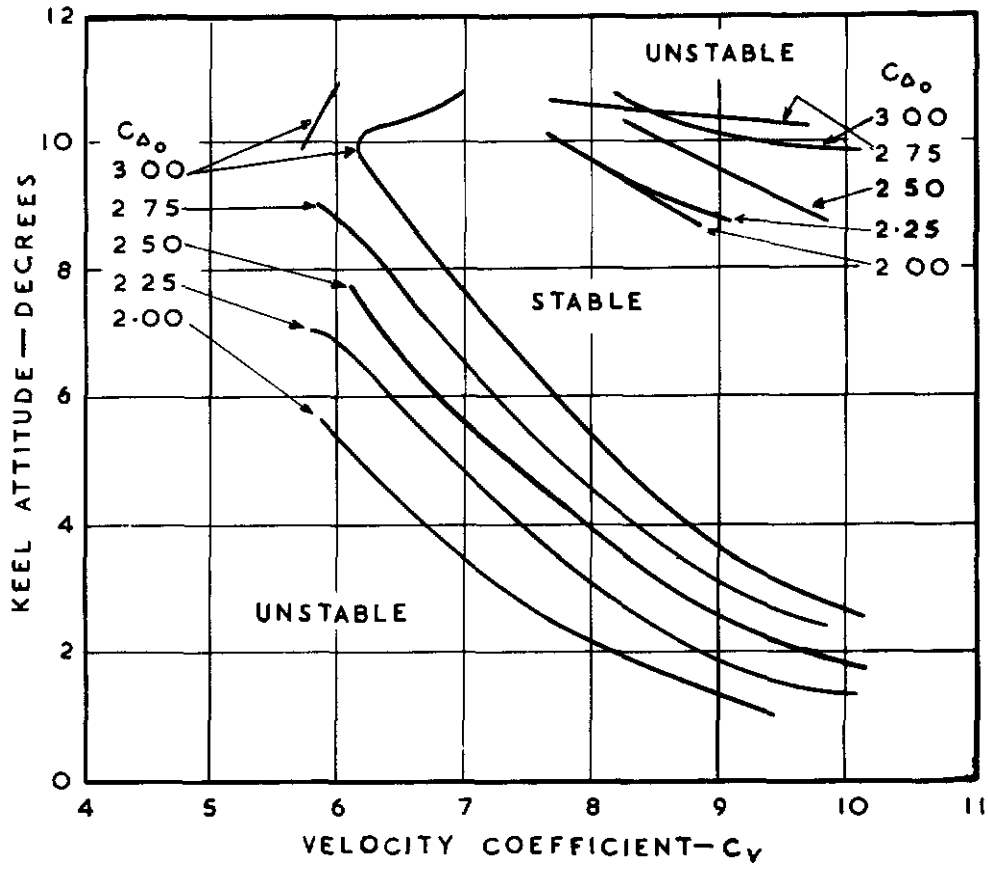

(A) ON A NON-DIMENSIONAL SPEED BASE

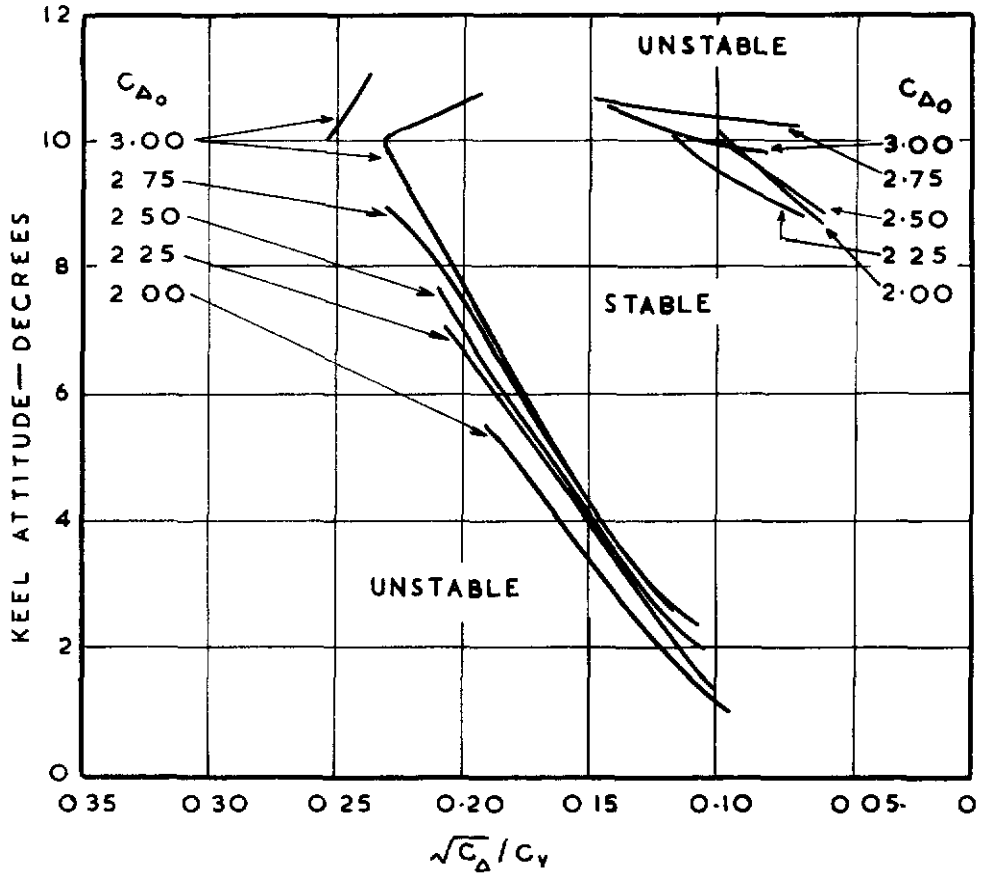

(B) ON A NON DIMENSIONAL $\sqrt{C_\Delta} / C_V$ BASE

MODEL B

LONGITUDINAL STABILITY LIMITS
AT DIFFERENT WEIGHTS

FIGS 17 & 18

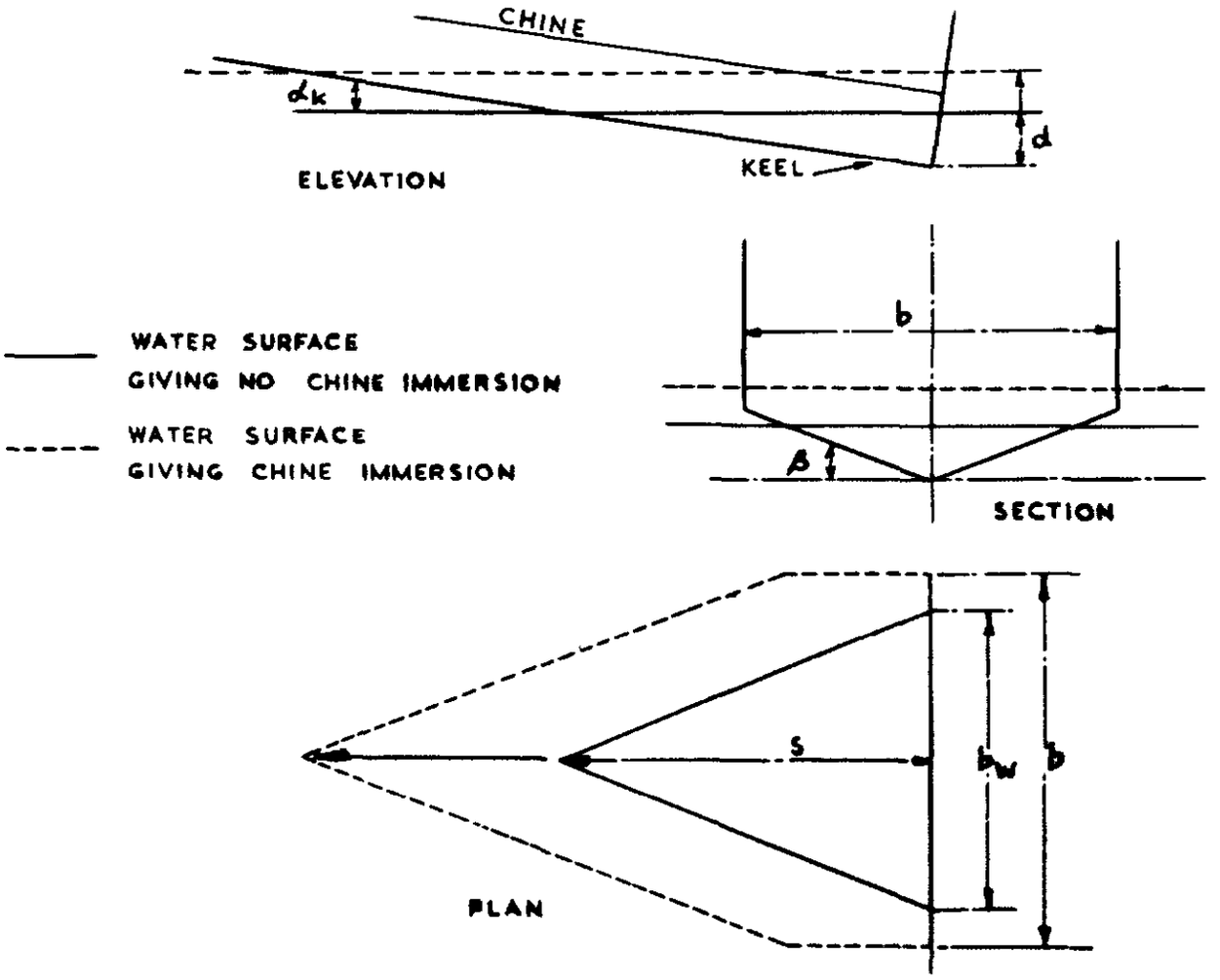

FIG 17 DIAGRAMMATIC ARRANGEMENT OF REPRESENTATIVE WEDGE

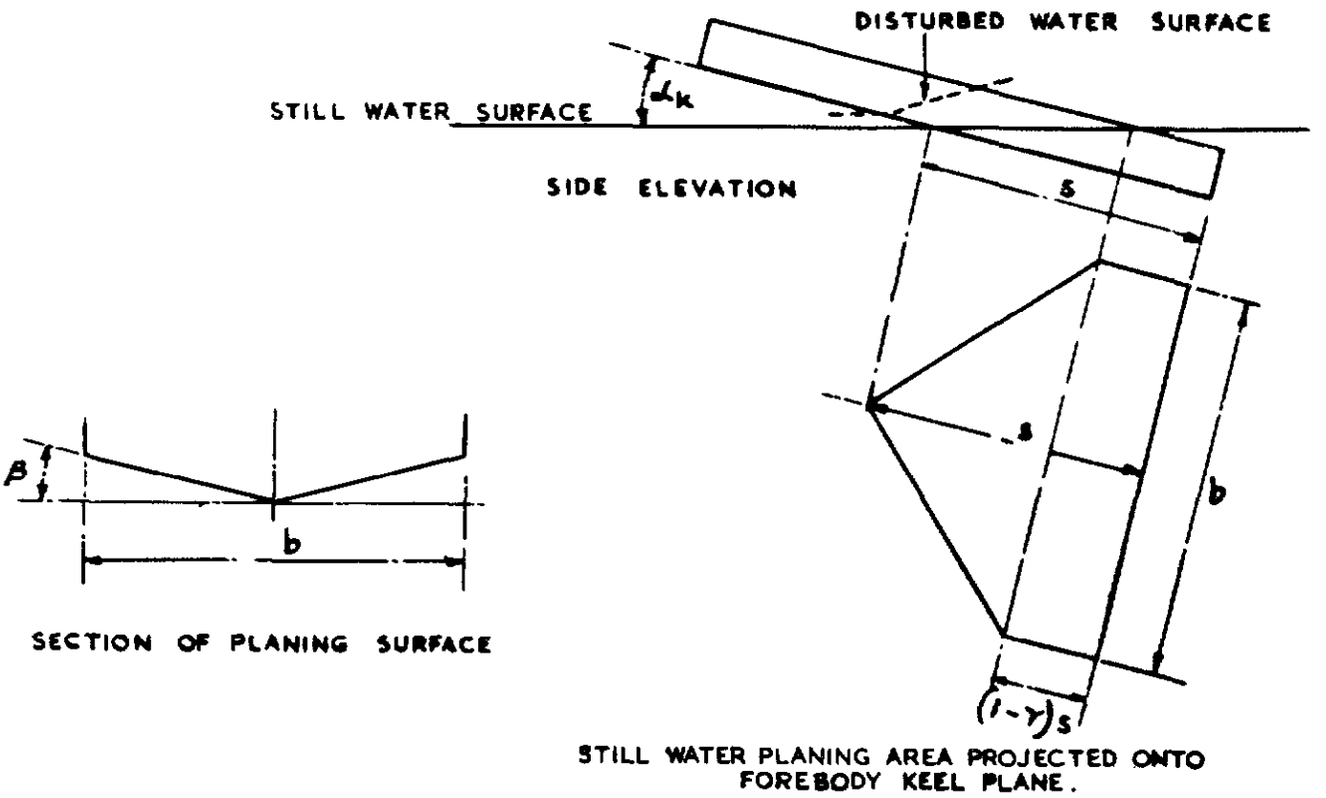

FIG 18 GEOMETRY FOR STILL WATER PLANING AREA

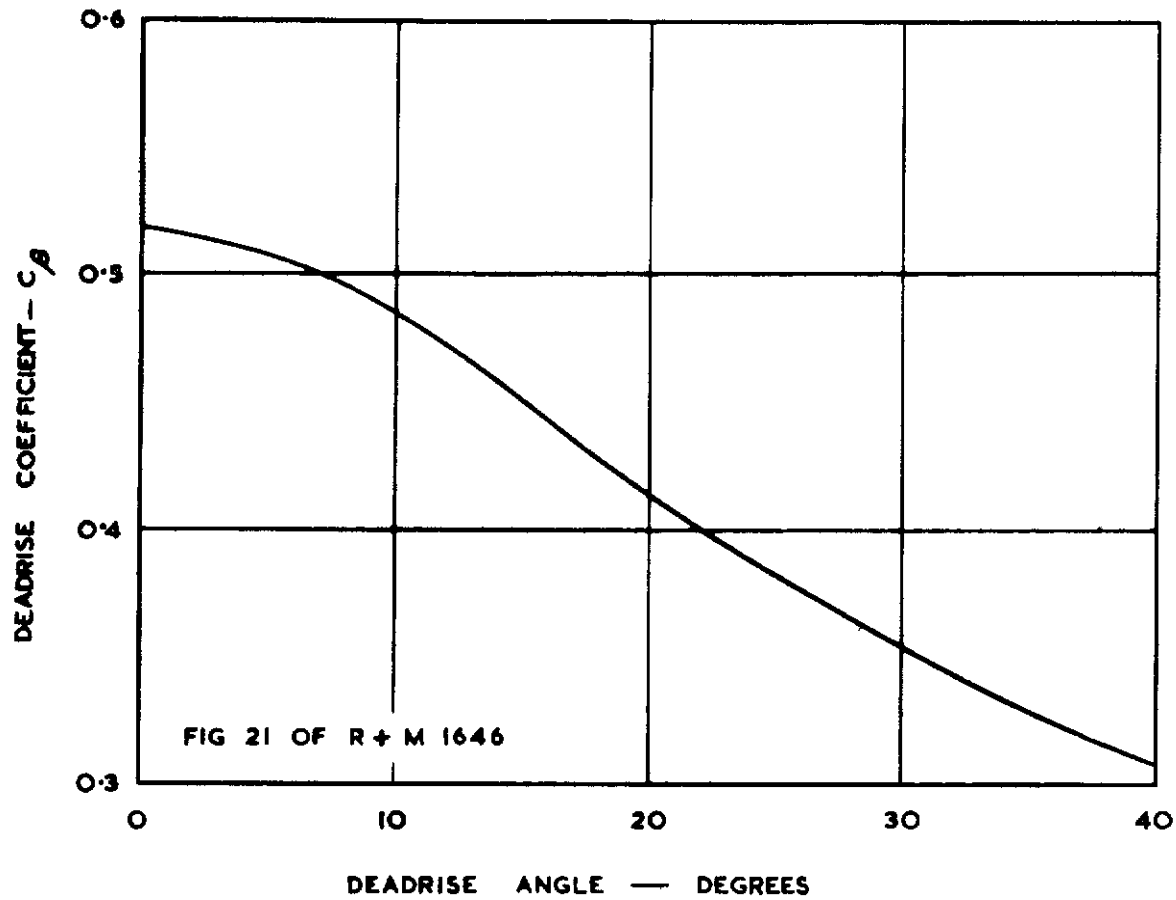

FIG 19 DEADRISE COEFFICIENT BASED ON WATERPLANE AREA

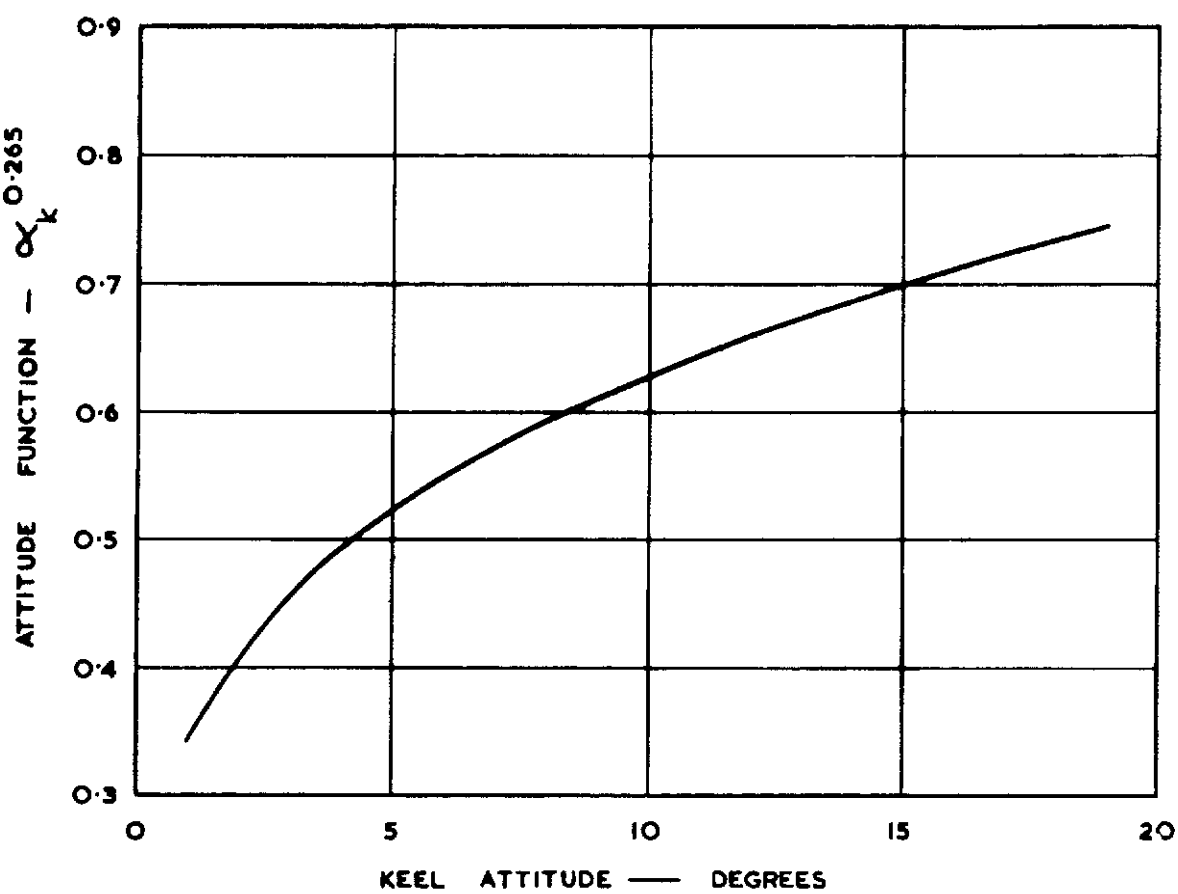

FIG 20 ATTITUDE FUNCTION FOR DRAUGHT PLOTTING

FIG 21

C_{Δ_0}	DRAUGHT EQUATION FOR LOWER STABILITY LIMIT
3·00	$d = 0{\cdot}051\,\alpha_K + 0{\cdot}99$
2·75	$d = 0{\cdot}057\,\alpha_K + 0{\cdot}97$
2·50	$d = 0{\cdot}065\,\alpha_K + 0{\cdot}96$
2·25	$d = 0{\cdot}074\,\alpha_K + 0{\cdot}94$

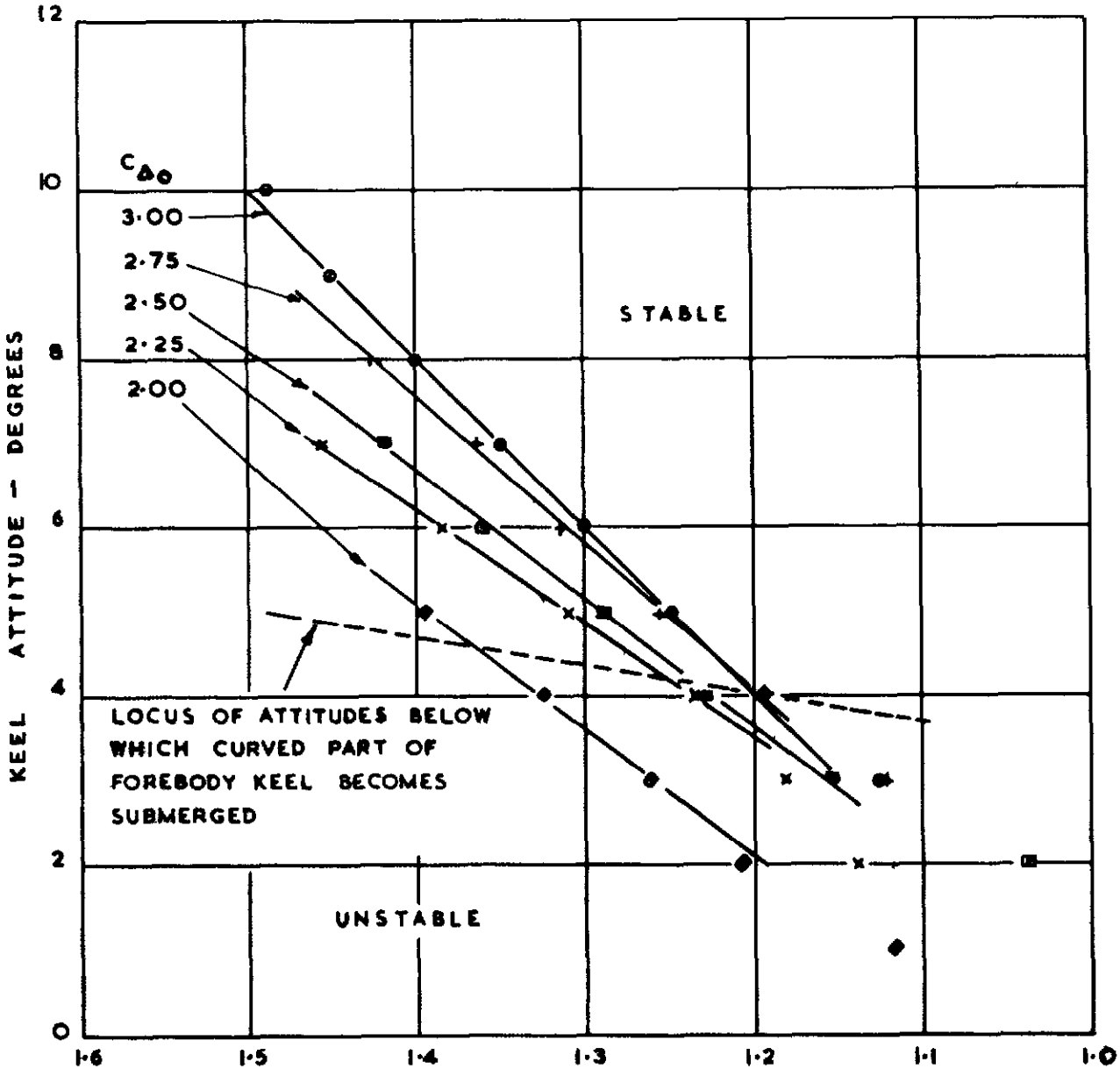

$$\text{DRAUGHT } d = \frac{\sqrt{C_\Delta}}{C_V} \cdot \frac{4{\cdot}06}{\alpha_K^{\,0{\cdot}265}} \text{ INS}$$

MODEL B

LOWER LONGITUDINAL STABILITY LIMITS AT DIFFERENT WEIGHTS ON A DRAUGHT BASE

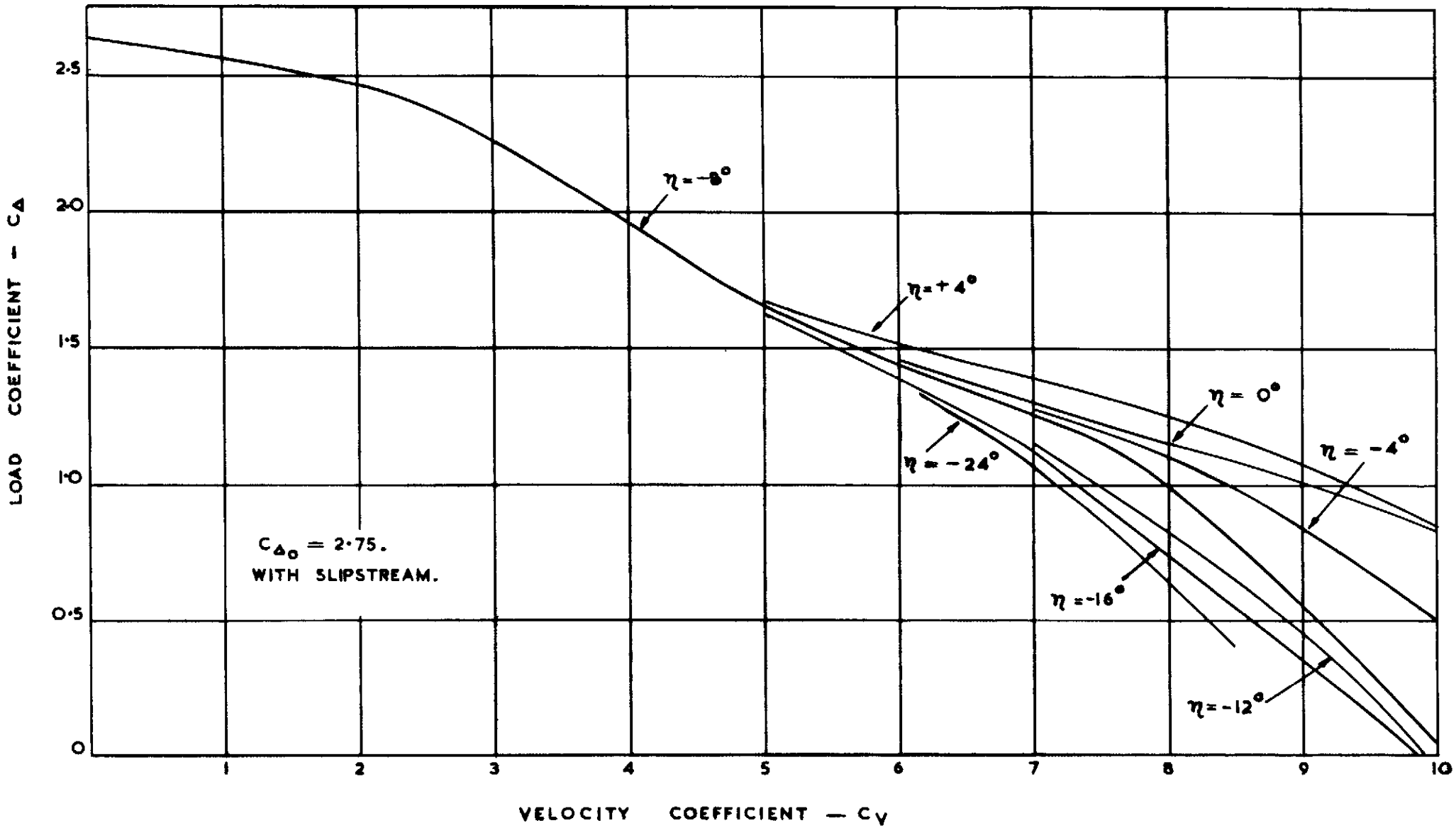

MODEL A

LOAD COEFFICIENT CURVES

FIG 22

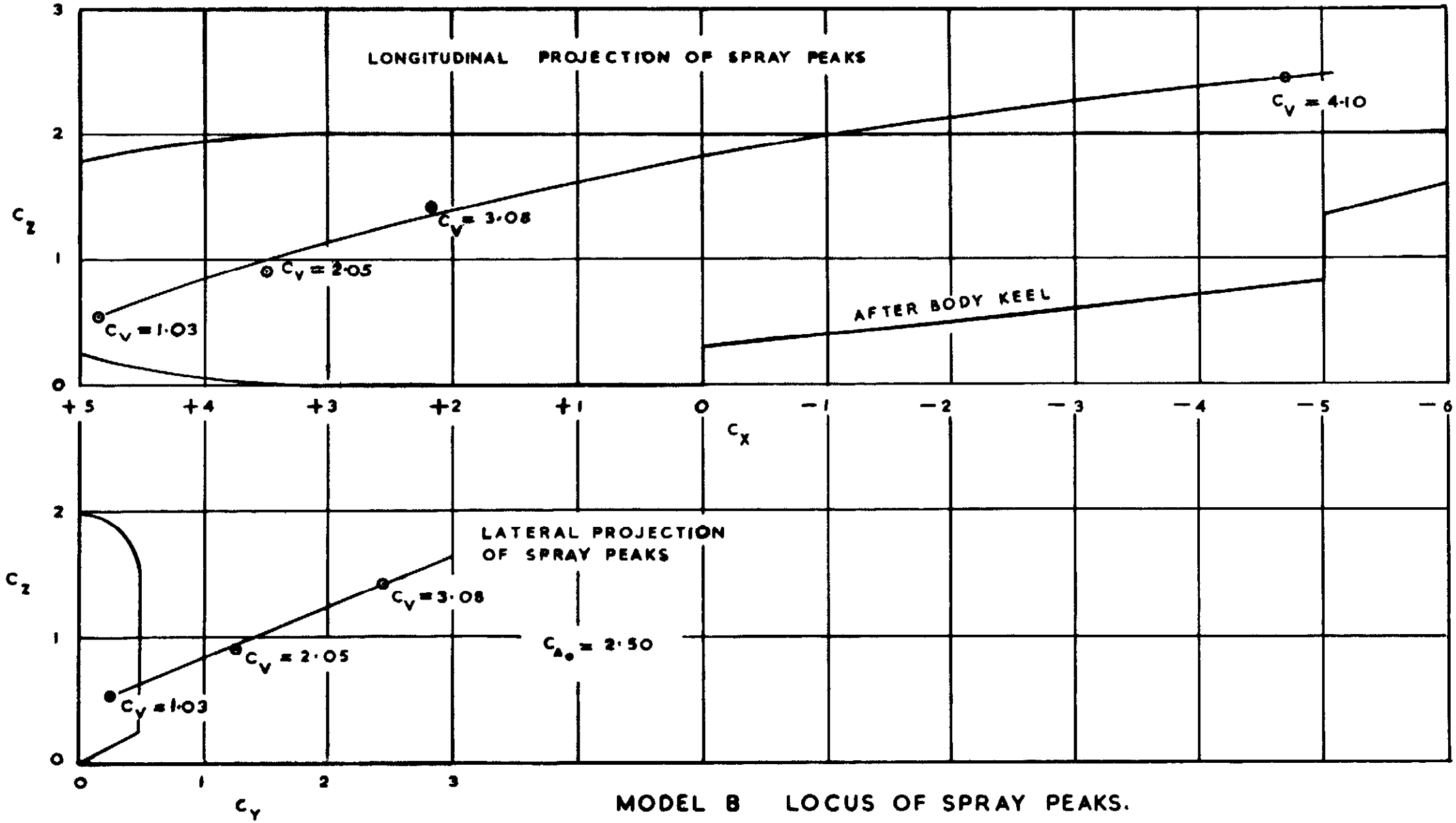

MODEL B LOCUS OF SPRAY PEAKS.

FIG 23

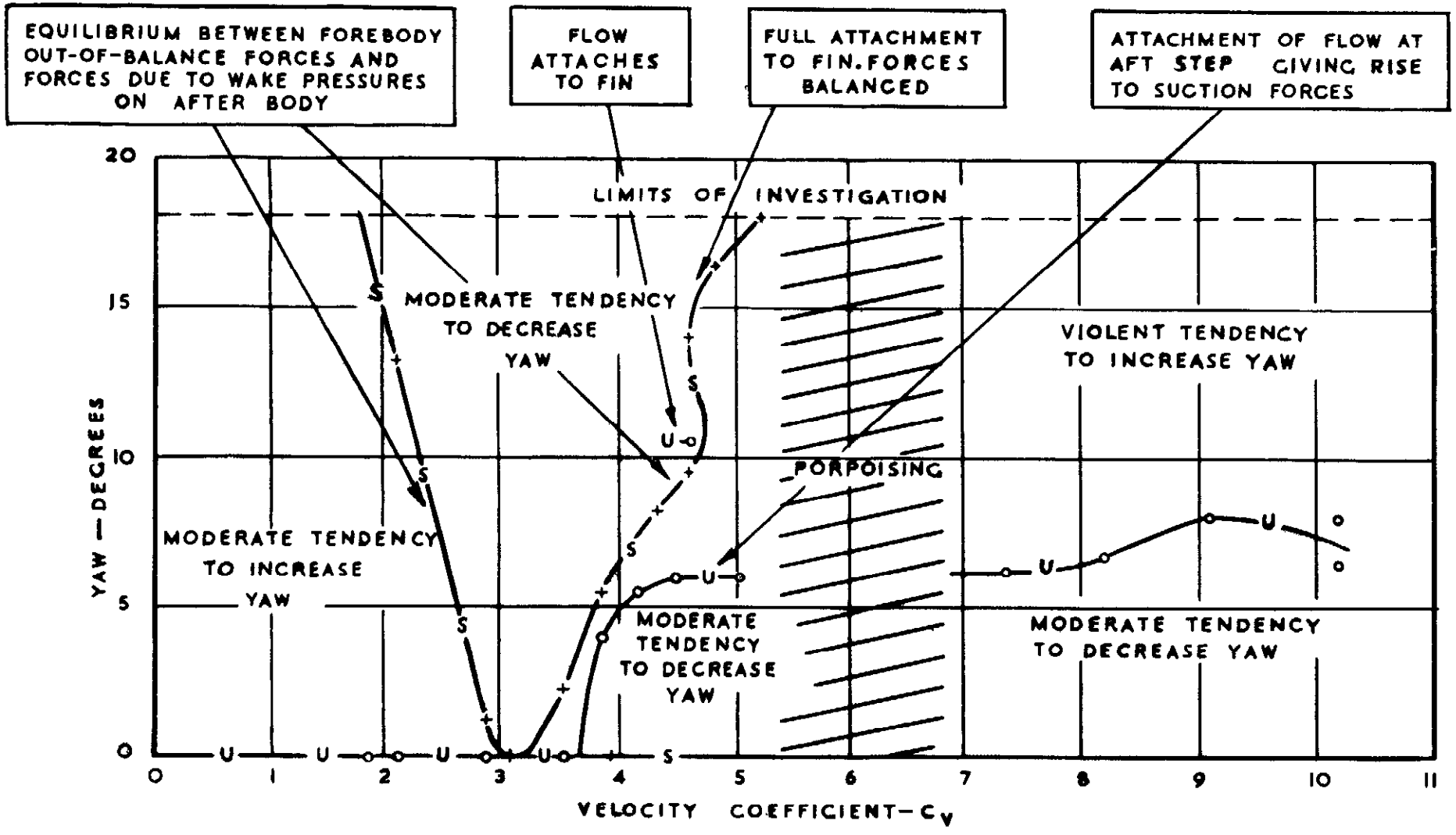

S = STABLE EQUILIBRIUM LINE
U = UNSTABLE EQUILIBRIUM LINE
$C_{\Delta_0} = 2.75$ $\eta = +2$ CONSTRAINED IN ROLL NO SLIPSTREAM

MODEL A
DIRECTIONAL STABILITY AT LOW PLANING ATTITUDES

FIG 24

FIG 25

C_{Δ_0} = 2·75 NO SLIPSTREAM

η = − 10° CONSTRAINED IN ROLL

S = STABLE EQUILIBRIUM LINE U = UNSTABLE EQUILIBRIUM LINE

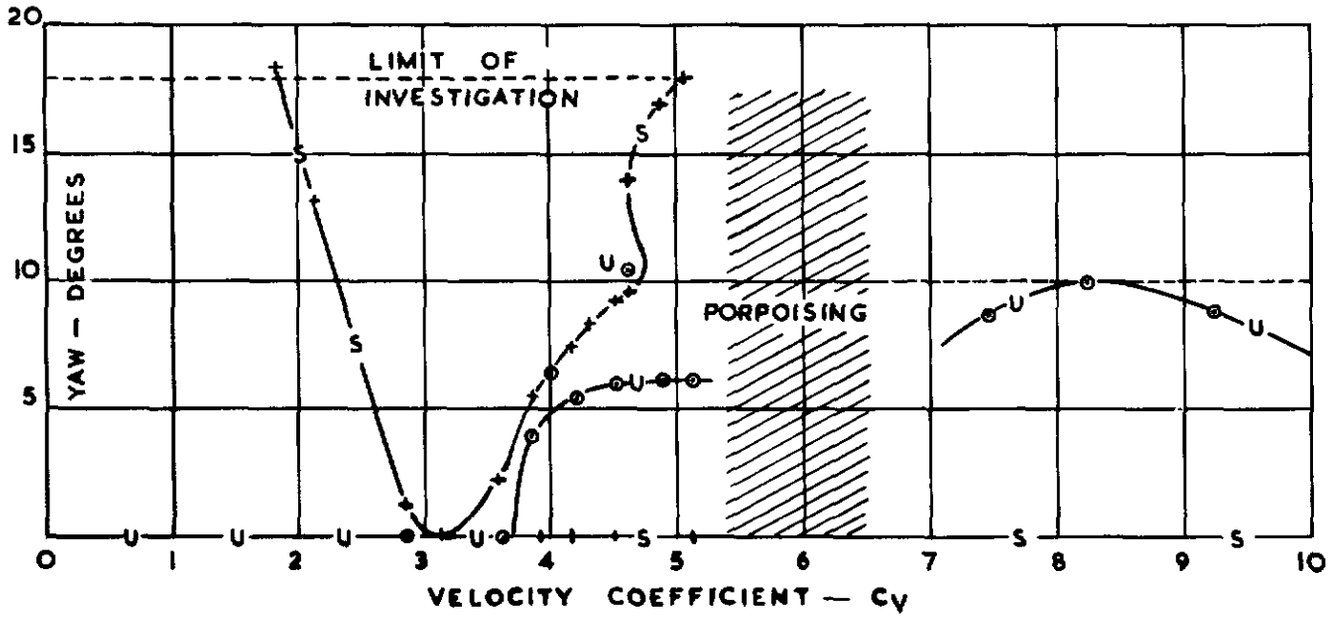

(A) WITHOUT BREAKER STRIPS

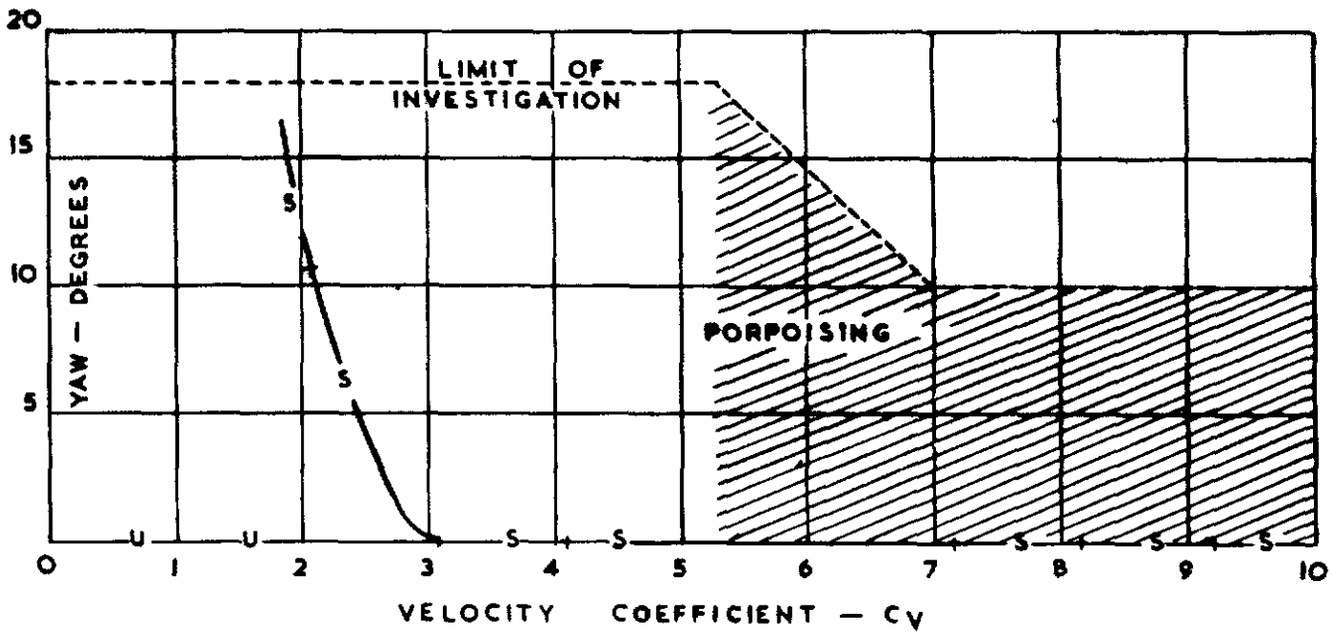

(B) WITH BREAKER STRIPS

MODEL A

DIRECTIONAL STABILITY AT HIGH PLANING ATTITUDES

FIG 26

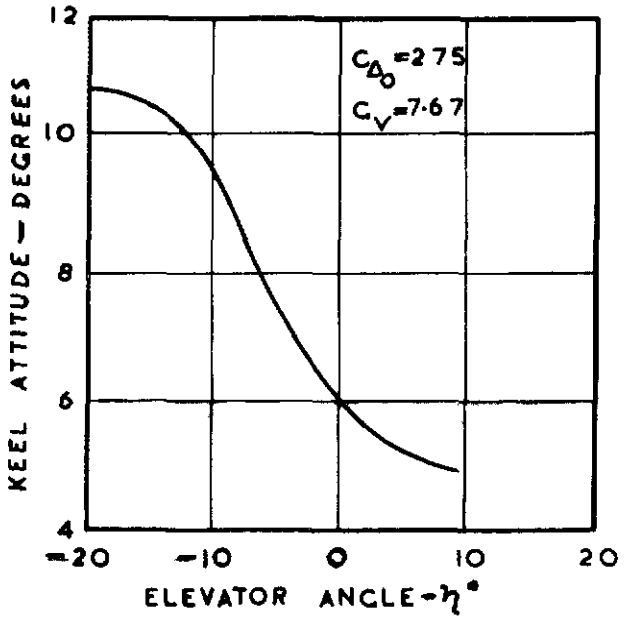

(A) VARIATION OF KEEL ATTITUDE WITH ELEVATOR ANGLE

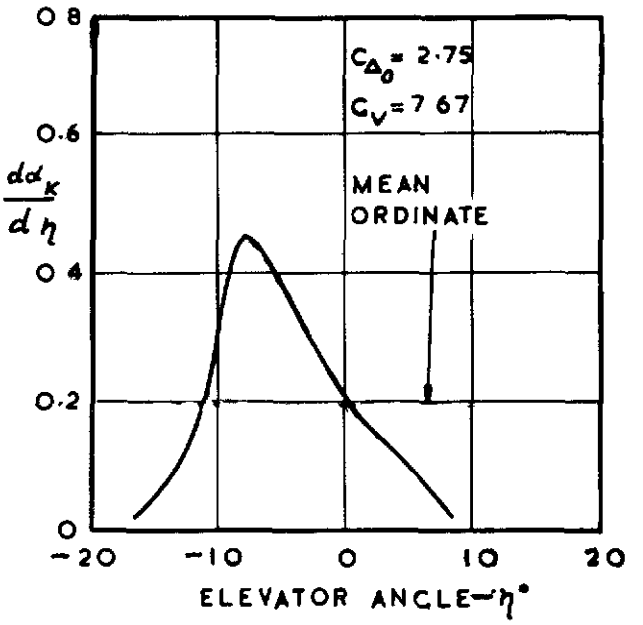

(B) SLOPE OF (A) WITH MEAN ORDINATE

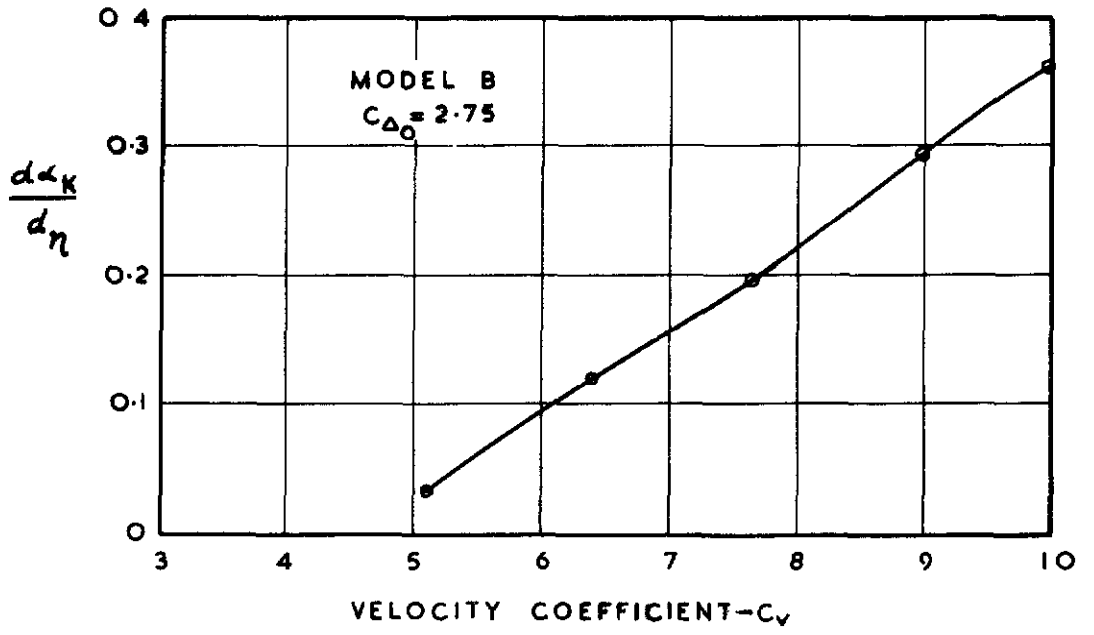

(C) FINAL PLOT SHOWING VARIATION OF ELEVATOR EFFECTIVENESS WITH VELOCITY COEFFICIENT

ELEVATOR EFFECTIVENESS

PRINTED AND PUBLISHED BY HER MAJESTY'S STATIONERY OFFICE

To be purchased from
York House, Kingsway, LONDON, W.C.2 — 423 Oxford Street, LONDON, W.1
P.O. Box 569, LONDON, S.E.1
13a Castle Street, EDINBURGH, 2 — 109 St. Mary Street, CARDIFF
39 King Street, MANCHESTER, 2 — Tower Lane, BRISTOL, 1
2 Edmund Street, BIRMINGHAM, 3 — 80 Chichester Street, BELFAST
or from any Bookseller

1955

Price 5s 0d net

PRINTED IN GREAT BRITAIN

S.O. Code No. 23-9009-1